AD-A146 395 EVALUATION OF THE RSTN (REGIONAL SEISMIC TEST NETWORK) 1/1
NETWORK AND FURTHE..(U) TELEDYNE GEOTECH ALEXANDRIA VA
ALEXANDRIA LABS R R BLANDFORD ET AL. 30 OCT 83
UNCLASSIFIED TGAL-TR-83-5 F08606-79-C-0007 F/G 8/11 NL

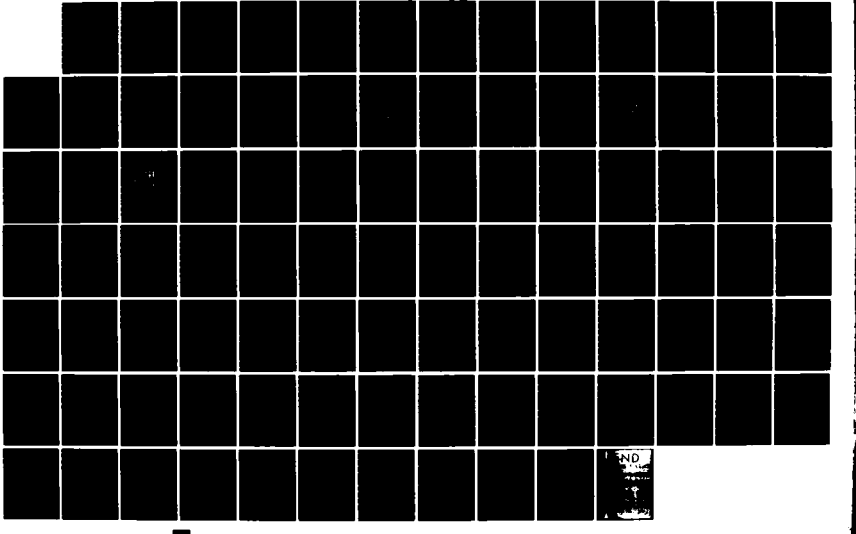

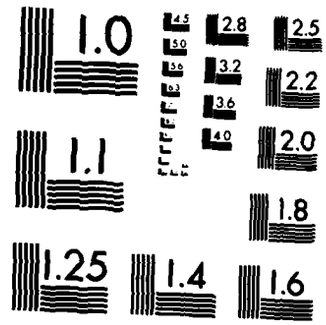
1.0
1.1
1.25
1.4
1.6
1.8
2.0
2.2
2.5
2.8
3.2
3.6
4.0
4.5
5.0
5.6

(12)

TGAL-TR-83-5

EVALUATION OF THE RSTN NETWORK AND FURTHER IMPROVEMENT TO AUTOMATIC ASSOCIATION

R.R. Blandford, J. Goncz, R. Baumstark, and K.L. McLaughlin

TELEDYNE GEOTECH
Alexandria Laboratories
314 Montgomery Street
Alexandria, VA 22314

30 October 1983

Technical Report

APPROVED FOR PUBLIC RELEASE, DISTRIBUTION UNLIMITED.

Prepared for:

DEFENSE ADVANCED RESEARCH PROJECTS AGENCY
1400 Wilson Boulevard
Arlington, VA 22209

Monitored by:

AFTAC/TG
Patrick Air Force Base
Florida 32925

Disclaimer: Neither the Defense Advanced Research Projects Agency nor the Air Force Technical Applications Center will be responsible for information contained herein which has been supplied by other organizations or contractors, and this document is subject to later revision as may be necessary. The views and conclusions presented are those of the authors and should not be interpreted as necessarily representing the official policies, either expressed or implied, of the Defense Advanced Research Projects Agency, the Air Force Technical Applications Center, or the US Government.

REPORT DOCUMENTATION PAGE

1a REPORT SECURITY CLASSIFICATION: Unclassified	1b RESTRICTIVE MARKINGS
2a SECURITY CLASSIFICATION AUTHORITY	3 DISTRIBUTION/AVAILABILITY OF REPORT: APPROVED FOR PUBLIC RELEASE; DISTRIBUTION UNLIMITED.
2b DECLASSIFICATION/DOWNGRADING SCHEDULE	
4 PERFORMING ORGANIZATION REPORT NUMBER(S): TGAL-TR-83-5	5. MONITORING ORGANIZATION REPORT NUMBER(S)
6a NAME OF PERFORMING ORGANIZATION: TELEDYNE GEOTECH Alexandria Laboratories; 6b. OFFICE SYMBOL (If applicable)	7a. NAME OF MONITORING ORGANIZATION: AFTAC/TG
6c ADDRESS (City, State and ZIP Code): 314 Montgomery Street Alexandria, Virginia 22314	7b. ADDRESS (City, State and ZIP Code): Patrick Air Force Base Florida 32925
8a NAME OF FUNDING/SPONSORING ORGANIZATION: DARPA; 8b. OFFICE SYMBOL (If applicable)	9. PROCUREMENT INSTRUMENT IDENTIFICATION NUMBER: F08606-79-C-0007
8c ADDRESS (City, State and ZIP Code): 1400 Wilson Boulevard Arlington, Virginia 22209	10. SOURCE OF FUNDING NOS: PROGRAM ELEMENT NO; PROJECT NO: VT/0709; TASK NO; WORK UNIT NO
11 TITLE (Include Security Classification): (See Block 16)	
12. PERSONAL AUTHOR(S): R. R. Blandford, J. Goncz, R. Baumstark, K. L. McLaughlin	
13a. TYPE OF REPORT: Technical; 13b. TIME COVERED: FROM 7/24/79 TO 10/30/83	14 DATE OF REPORT (Yr., Mo., Day): October 30, 1983; 15 PAGE COUNT: 92
16. SUPPLEMENTARY NOTATION: EVALUATION OF THE RSTN NETWORK AND FURTHER IMPROVEMENTS TO AUTOMATIC ASSOCIATION	

17 COSATI CODES		
FIELD	GROUP	SUB. GR.
08	11	

18. SUBJECT TERMS (Continue on reverse if necessary and identify by block number): RSTN, Detection, Threshold, m_b, Lg, LR, Automatic Association, pP, Earthquake Location

19 ABSTRACT (Continue on reverse if necessary and identify by block number)

A review of 9 North American events was used to evaluate available RSTN data at the CSS. Signal-to-noise ratios in the time and frequency domains were used to estimate detection thresholds for P, Lg and L_R at regional distances. The P detection threshold at $\Delta \sim 10°$ is near $M_L = 3$. L_g detection thresholds were found to be lower than the P detection thresholds for distances greater than 15 degrees by approximately 0.5 M_L. LR detection thresholds are nearly flat near $M_L \sim 3.5$ for $\Delta < 30°$. Due to the small number of events examined, these results are preliminary estimates of detection thresholds. Additional work should investigate the actual detection of small events at regional distances using a larger data base and automated techniques.

20 DISTRIBUTION/AVAILABILITY OF ABSTRACT: UNCLASSIFIED/UNLIMITED ☒ SAME AS RPT ☐ DTIC USERS ☐	21 ABSTRACT SECURITY CLASSIFICATION: Unclassified	
22a NAME OF RESPONSIBLE INDIVIDUAL: 1Lt Kenneth M. Ols	22b TELEPHONE NUMBER (Include Area Code): 305-494-5263	22c OFFICE SYMBOL: TGR

DD FORM 1473, 83 APR EDITION OF 1 JAN 73 IS OBSOLETE

19) Continued

Further improvements to Automatic Association, AA, have been made to incorporate amplitude data, two array event location, depth phase constraints, unassociated arrivals, and confidence ellipsoids. Two event array location, unassociated arrivals and confidence ellipsoids are completed and help to improve the usefulness and readability of the summary event bulletin. Work on depth phase constraints was evaluated with synthethic arrival data and needs further investigation with real data. Incorporation of amplitude data yields a maximum likelihood estimate of m_b and helps to define a good event and to reject spurious events. It requires more station information (diurnal noise, m_b bias) than is available for many seismic recording systems, however. Its utilization requires that this information be included for each seismic network that AA is applied to.

ABSTRACT

A review of 9 North American events was used to evaluate available RSTN data at the CSS. Signal-to-noise ratios in the time and frequency domains were used to estimate detection thresholds for P, Lg and L_R at regional distances. The P detection threshold at $\Delta \sim 10°$ is near $M_L = 3$. L_g detection thresholds were found to be lower than the P detection thresholds for distances greater than 15 degrees by approximately 0.5 M_L. LR detection thresholds are nearly flat near $M_L \sim 3.5$ for $\Delta < 30°$. Due to the small number of events examined, these results are preliminary estimates of detection thresholds. Additional work should investigate the actual detection of small events at regional distances using a larger data base and automated techniques.

Further improvements to Automatic Association, AA, have been made to incorporate amplitude data, two array event location, depth phase constraints, unassociated arrivals, and confidence ellipsoids. Two event array location, unassociated arrivals and confidence ellipsoids are completed and help to improve the usefulness and readability of the summary event bulletin. Work on depth phase constraints was evaluated with synthethic arrival data and needs further investigation with real data. Incorporation of amplitude data yields a maximum likelihood estimate of m_b and helps to define a good event and to reject spurious events. It requires more station information (diurnal noise, m_b bias) than is available for many seismic recording systems, however. Its utilization requires that this information be included for each seismic network that AA is applied to.

(THIS PAGE INTENTIONALLY LEFT BLANK)

TABLE OF CONTENTS

LIST OF FIGURES

LIST OF FIGURES (Continued)

LIST OF FIGURES (Continued)

LIST OF TABLES

(THIS PAGE INTENTIONALLY LEFT BLANK)

EVALUATION OF THE RSTN NETWORK

Introduction

The Regional Seismic Test Network (RSTN) is a 5-station seismic network designed to monitor regional seismicity on the scale of a large continental shield. The RSTN serves as a prototype for a network that could be deployed for test ban treaty verification. Both regional and teleseismic signals are digitally recorded for three components of earth motion in three overlapping frequency bands covering 0.02 to 10 Hz. The instruments, signal conditioning, and recording facilities are discussed in Rodgers and Hammel (1981), and Breding (1982).

Each station consists of a three component broadband Teledyne Geotech KS-36000 and a high frequency Teledyne Geotech S-750 in a borehole at a depth of 100 meters. The KS-36000 output signals are processed to yield a long period band, an intermediate period band, and a short period band (see Figure 1). The digital data is transmitted by satellite to the System Control and Receiving Station in Albequerque, N. M. (SCARS), and the Center for Seismic Studies (CSS) in Arlington, Va., as well as other sites in North America. The data used in this report was partly received at CSS and partly recorded at SCARS. A description of RSTN station localities is contained in Taylor and Qualheim (1983). All RSTN stations are located on Precambrian or Paleozoic sediment at "hard rock" sites of the Canadian Shield. The network spans nearly 27° of latitude and 40° of longitude (Figure 2).

Because the RSTN is a sparse network of three-component "broadband" stations it poses unique problems in the task of developing a regional system of automatic detection and association. The P_n, Pg, Sn, Lg regional phases have not been incorporated into a detection, location, and association process. Three-component stations with three frequency bandwidths offer the opportunity to determine the optimal frequency bands for detection and identification of these phases. Regional detection becomes substantially important in the context of a CTBT because of agreements between the USA and USSR that internal 3-component stations could be implemented in the event of such a treaty.

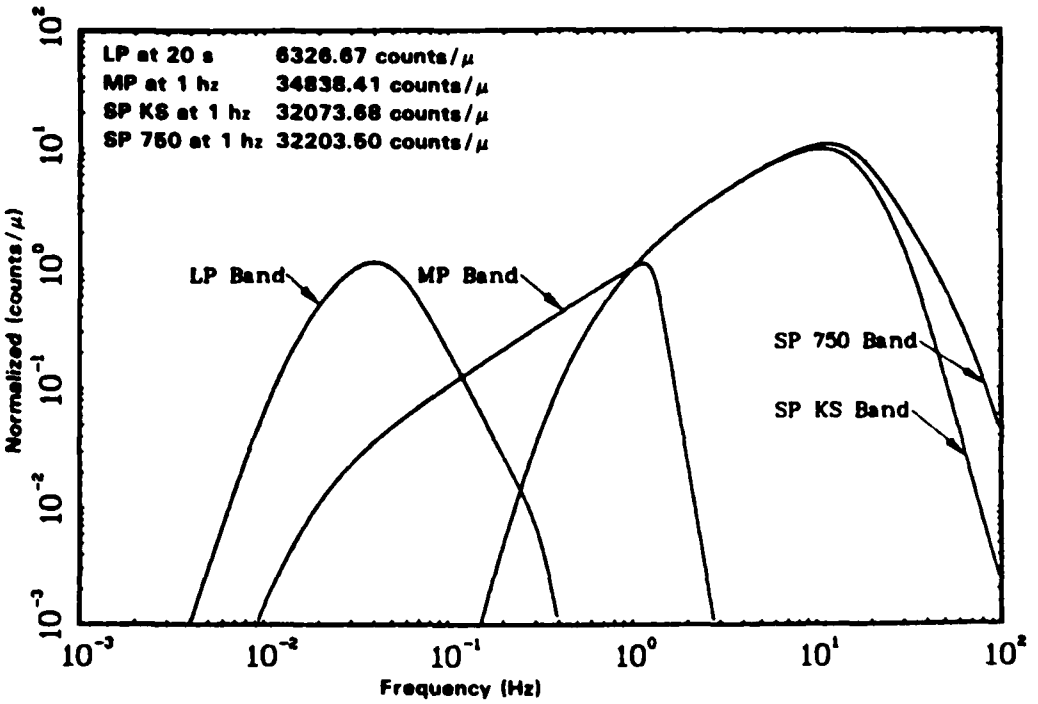

Figure 2.7 RSTN Normalized Displacement Amplitude Responses

Figure 1 RSTN Normalized displacement response from Breding (1982)
LP: long period band recording
MP: middle period band recording
SPK: short period band KS-36000 recording
SP7: short period band S-750 recording

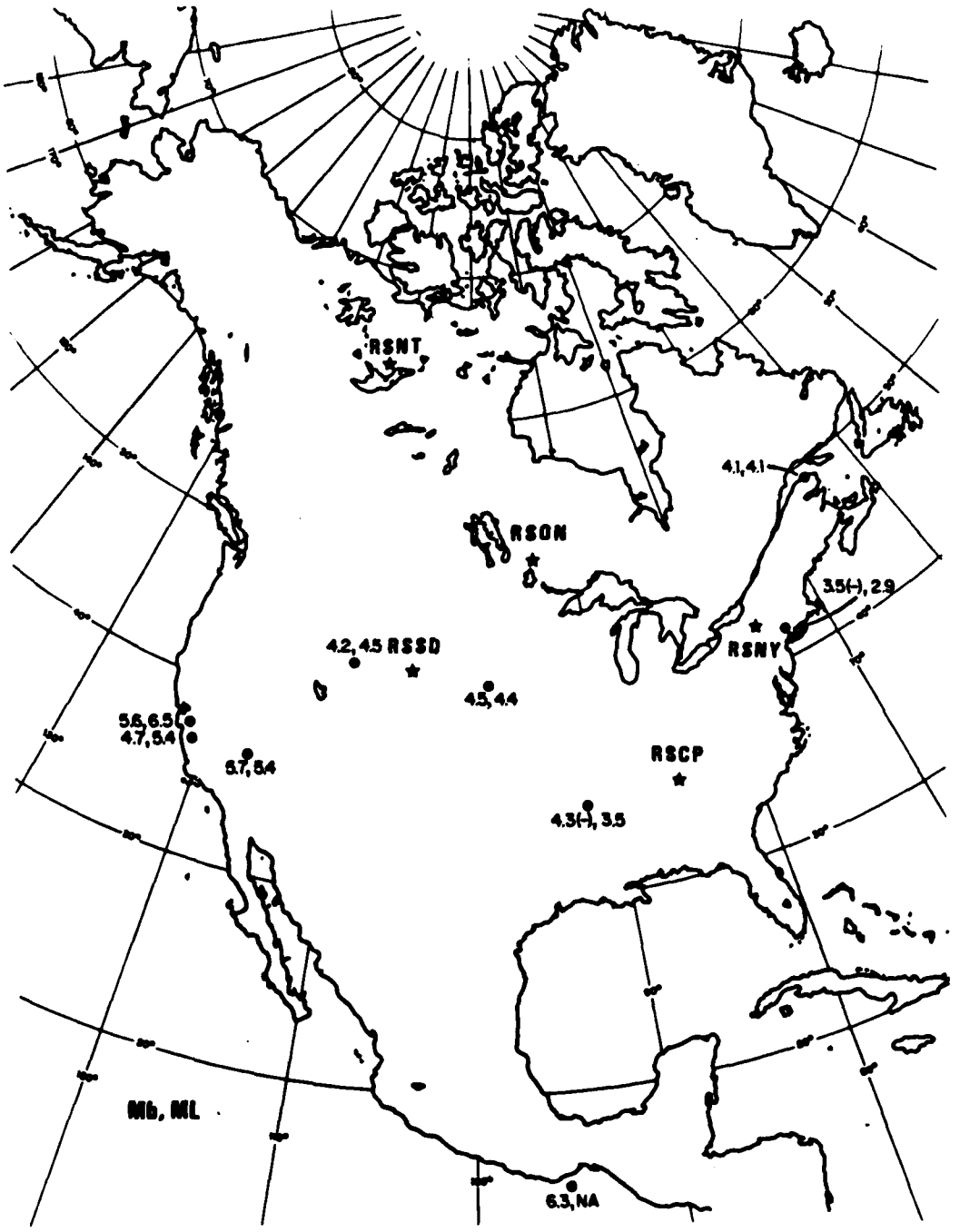

Figure 2 Location of events examined in this report (see Table I) and RSTN station locations M_B and M_L are shown for each event.

TABLE I

Event Location

	M_L	NAME	#	LAT(N)	LON(W)	OT	DATE	M_B
	5.4	NTS	1	37	116	14:00	82/217	5.7
	5.4	CALONE	2	36.3	120.5	22:26	82/298	4.7
	3.5	ARK	3	35.1	92.2	02:30	83/019	4.3
	4.5	YELLOW	4	44.5	110.6	20.25	83/037	4.2
	6.5	CAL	5	36.2	120.3	23:42	83/122	5.6
	4.1	GASPE	6	49.1	67.0	19:35	83/017	4.1
	2.9	NY	7	41.5	73.6	19:59	83/057	3.5
(M_B)	6.3	MEX	8	16.1	95.2	08:17	83/024	5.7
	4.4	DAKOTA	9	44.2	99.4	06:32	83/065	4.5

TABLE II

RSTN Station Locations

RSTN	Lat	Long	Elev
RSNY (New York)	44°32'54"N	74°31'48"W	457m
RSCP (Cumberland Plateau)	35°36'00"N	85°34'08"W	581m
RSSD (South Dakota)	44°07'13.5"N	104°02'10.3"W	2060m
RSON (Ontario)	50°51'32"N	93°42'08"W	405m
RSNT (North West Territories)	62°28'47"N	114°35'30"W	191m

The approach of this study was to select 9 events recorded by the network and manually analyze the recordings using available software at the CSS (Table I, and Figure 2). Various phases were identified and "picked" as well as possible, back azimuths were estimated, and signal-to-noise ratios were determined. Finally, detection thresholds as a function of distance were estimated for P, Lg and L_R phases using the signal-to-noise ratios of the 9 events. Several existing CSS software packages were tested using the RSTN evaluation data. In the course of data analysis the quality of RSTN data was examined. Due to deficiencies in both data quality and available software, some intended tasks could not be performed on the RSTN data. These tasks were subject to the programming and computational priorities of the CSS activities. Data analysis was supported with programs described in Lincoln Lab manual 132 and standard UNIX software. Several "bugs" were found and corrected in the existing software. Also, short digital "drop-outs" detected in the data required additional changes to the existing software to locate and correct the data drop-outs.

Data Analysis

The following discussion serves to illustrate the analysis performed at the CSS with examples from the RSTN data used in this report.

Figure 3 shows the NTS event, day 217 of 1982, recorded at RSSD. The distance is 11.49°. From top-to-bottom are 40 seconds of three-component short period data, 375 seconds of three-component middle period data, and 1500 seconds of long period data. The P wave is emergent on the short period components with strong radial polarization. The measured apparent azimuth from the horizontal components is within 2 degrees of the computed back azimuth to the event. Lg is clearly visible on the middle period band and L_R is well recorded on the long period band. Although the P arrival is well recorded on the middle period band, the P wave train is not detectable in the time domain on the long period band. The time windows used for spectral estimation of the P wave are indicated with vertical bars labeled "start" and "end". Amplitude signal-to-noise ratios (S/N) were estimated in the time domain and in the frequency domain. The results are tabulated in Appendix I for each event, station, and signal channel. The time domain maximum amplitude S/N was estimated for the short period Z, N, and E components as 98, 73, and 85 respectively. The predominant periods were 0.2, 0.18 and 0.15 seconds on the respective Z, N, and E components.

Figures 4a and 4b are plots of the short period and middle period channel P-wave amplitude spectra for the windows indicated in Figure 3. The noise estimate (dashed line) is computed from a window of the same length for each component directly preceeding the P wave arrival. All spectra in this report are shown as amplitude spectra uncorrected for instrument. The maximum S/N was estimated from each plot as 450, 250, and 525 at 1.1 Hz on the short period band and 466, 350, and 350 at .9 to 1.1 Hz on the middle period band. The long period band P-wave has no significant signal above the noise. The P-wave spectra in Figure 4b are asymptotic to the noise level at 0.2 Hz. This was common at all RSTN stations. A long period explosion P wave null is indicated by the time domain and spectral domain estimates of the P-wave signal strength.

NTS, RSSD
Δ° = 11.49

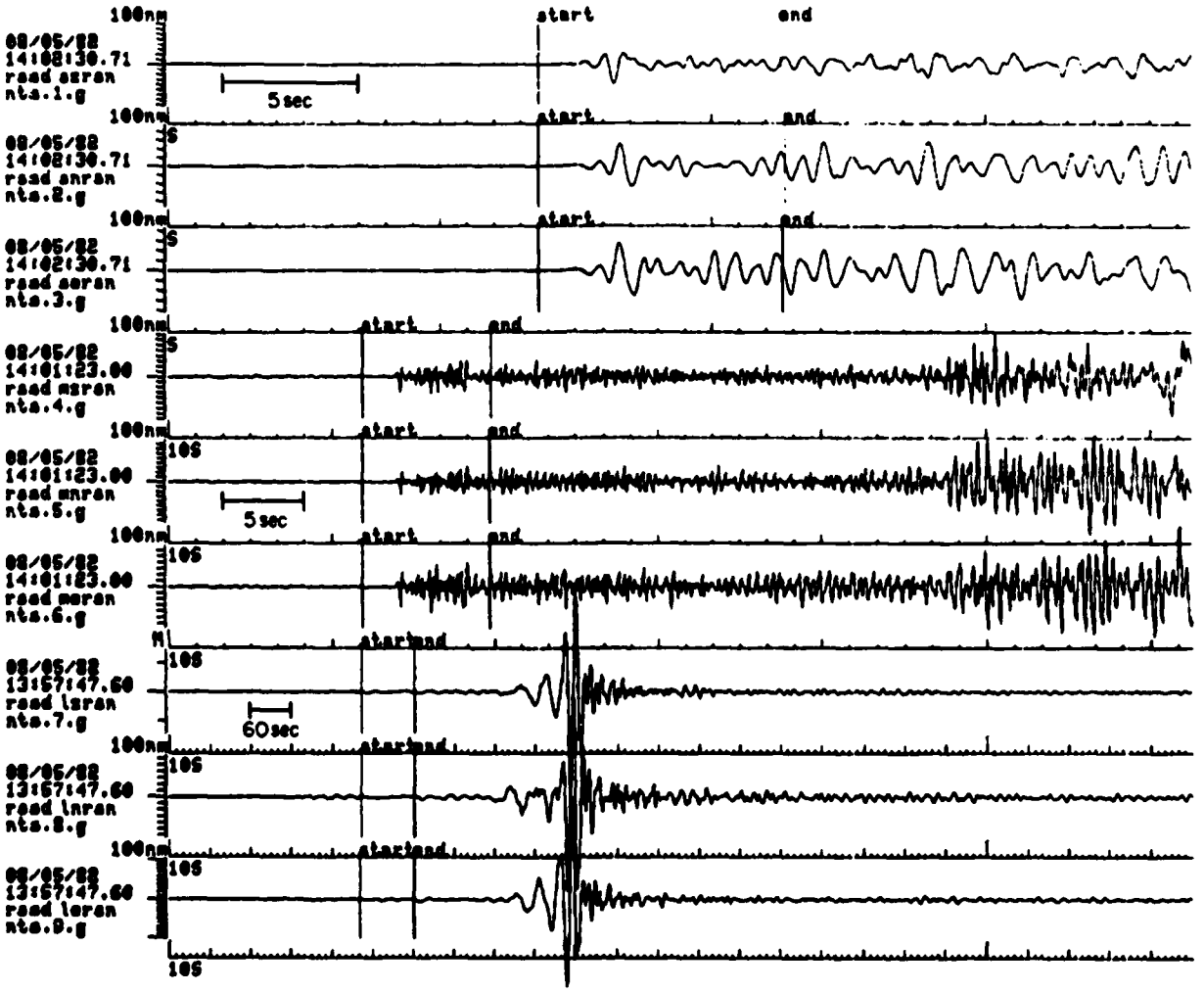

Figure 3 NTS-to-RSSD (11.49°) from top to bottom: Short period Z,N,E (40 seconds) Mid period Z,N,E (375 seconds) and Long period Z,N,E (1500 seconds) The vertical scale tick marks are 100nm for each trace, except the long period Z. The tick marks for the LPZ are 1 micron increments. The P wave window for spectral estimation in Figure 4 is shown on each seismogram indicated by the vertical bars labeled "start" and "end". Noise windows were selected prior to the P arrival. The P_n character of P is clear on the short period Z with strong radial polarization. Lg is clearly observable on the Mid period band and L_R is well recorded on the long period band. The P wave is not detectable on the long period.

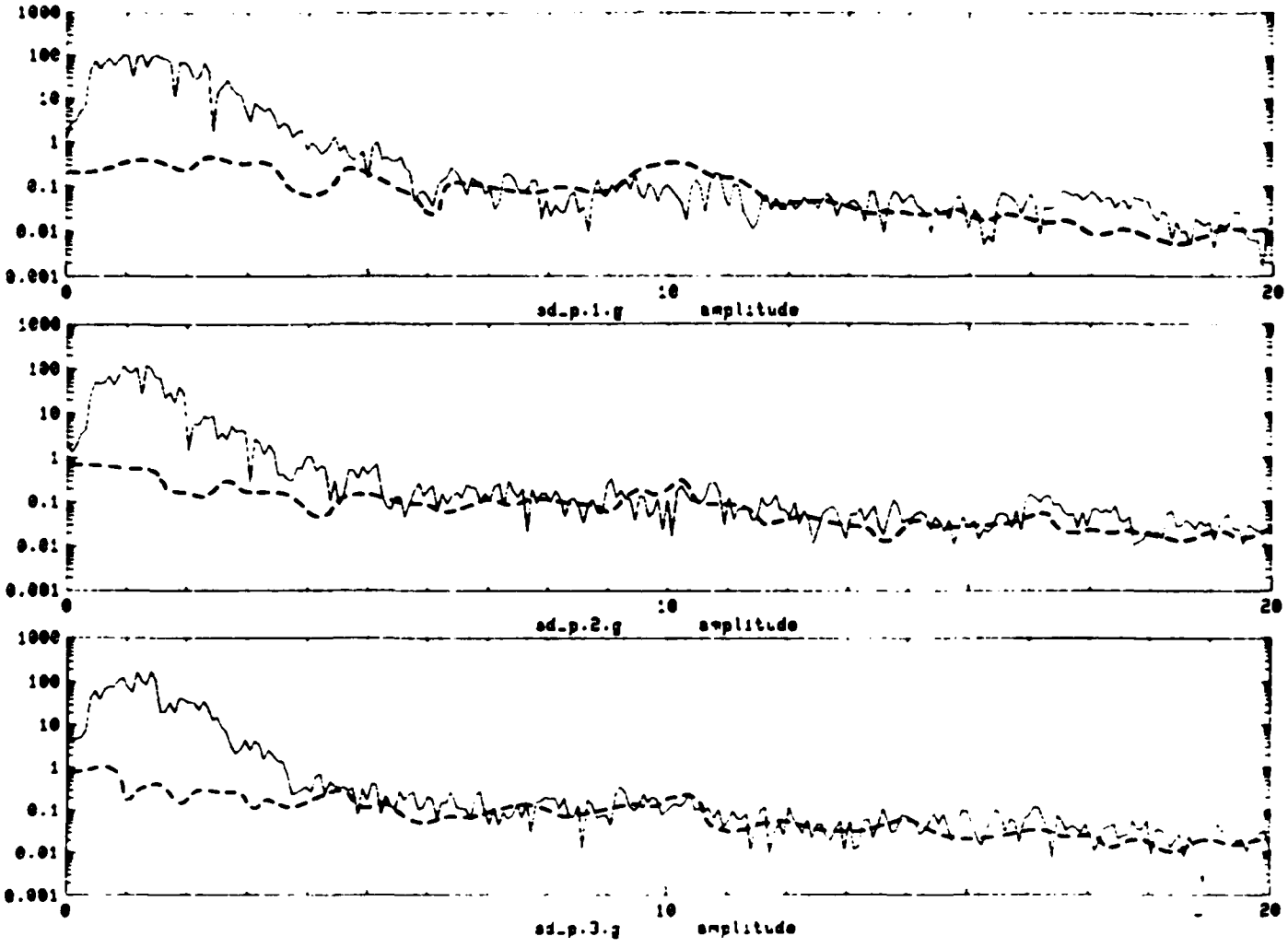

Figure 4A NTS-to-RSSD (11.49°) short period 3-component P wave amplitude spectra with noise spectra superimposed. Units are nm-(sec)$^{1/2}$ at 1 Hz. Spectra are not corrected for frequency dependent instrument response. Signal-to-noise ratio is estimated as 450, 250, and 525 on Z,N,E respectively all at 1.1 Hz.

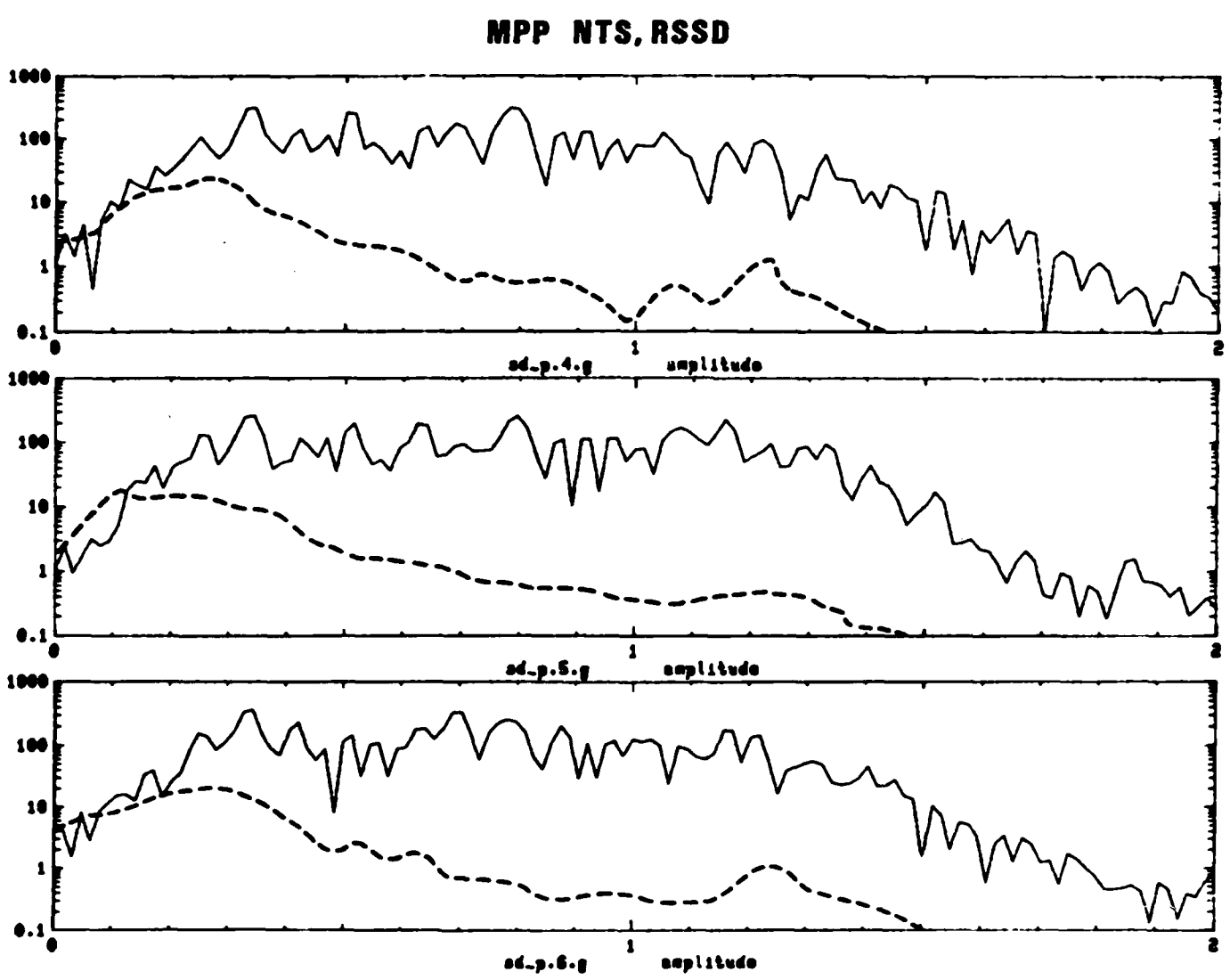

Figure 4B NTS-to-RSSD (11.59°) Mid period 3-component amplitude spectra with noise spectra superimposed. Signal-to-noise is estimated as 566, 350, and 350 on Z,N,E at .98, 1.12, and .9 Hz respectively. Spectra are asymptotic to noise levels at frequencies below 0.20 Hz, indicative of a long period P wave null. Units are nm-(sec)$^{1/2}$ at 1 Hz. Spectra are uncorrected for frequency dependent instrument response.

For comparison with the explosion traces of Figure 3, the California earthquake of 10/25/82, M_L 5.4 (Δ= 14.78°), is shown in Figure 5a. The initial short period P-wave appears with much the same signal-to-noise ratio as the NTS event, while the long period P-wave is clearly visible on the bottom three traces. Love and Rayleigh waves are clearly seen on the long period records. S waves are apparent on both middle and long period band records. In Figures 5b and C, P-wave middle period and long period spectra are observed above the noise at frequencies below 0.1 Hz at this distance and magnitude level for earthquakes.

Lg signal-to-noise ratios are estimated in much the same way as P-wave signal-to-noise estimates. Figure 6a demonstrates the short period Lg spectra of the NTS event at RSSD (Δ = 11.49°) and Figure 6b illustrates the same on the middle period band records. Lg has similar amplitudes on all three components of motion. The maximum signal-to-noise ratio for Lg was found at 0.5 to 0.7 Hz on both short period and middle period channels. Similarly, the long period L_R signals are presented in Figure 7.

As an example of a shorter intra-shield propagation path, the Dakota earthquake recorded at RSSD (Δ= 3.3°) is shown in Figure 8. There is a well developed Pg-Pn separation of 8 seconds on the short and middle period bands. Propagation is from the east (87°) and the P wavetrain is best observed on the vertical and east components. S waves and Lg are well developed on the middle period band. A broadband pulse of superimposed S and surface waves is prominent on the long period records.

In contrast to the NTS P-wave spectra at RSSD (Figure 4a) the spectra of the Dakota earthquake in Figures 9a and b are above the noise to the Nyquist frequencies at 20 Hz and 2 Hz. Some aliasing may be present.

At this point we should point out some aspects of the short-period noise spectra. In Figures 4a and 6a the "noise" spectra are all nearly flat between 6 and 10 Hz. This is common for RSSD. Between 10 and 20 Hz the level declines to .01 mμ. The spectra have not been corrected for instrument response and the high frequency level corresponds to a

CALONE, RSSD
$\Delta^{\circ} = 14.78$

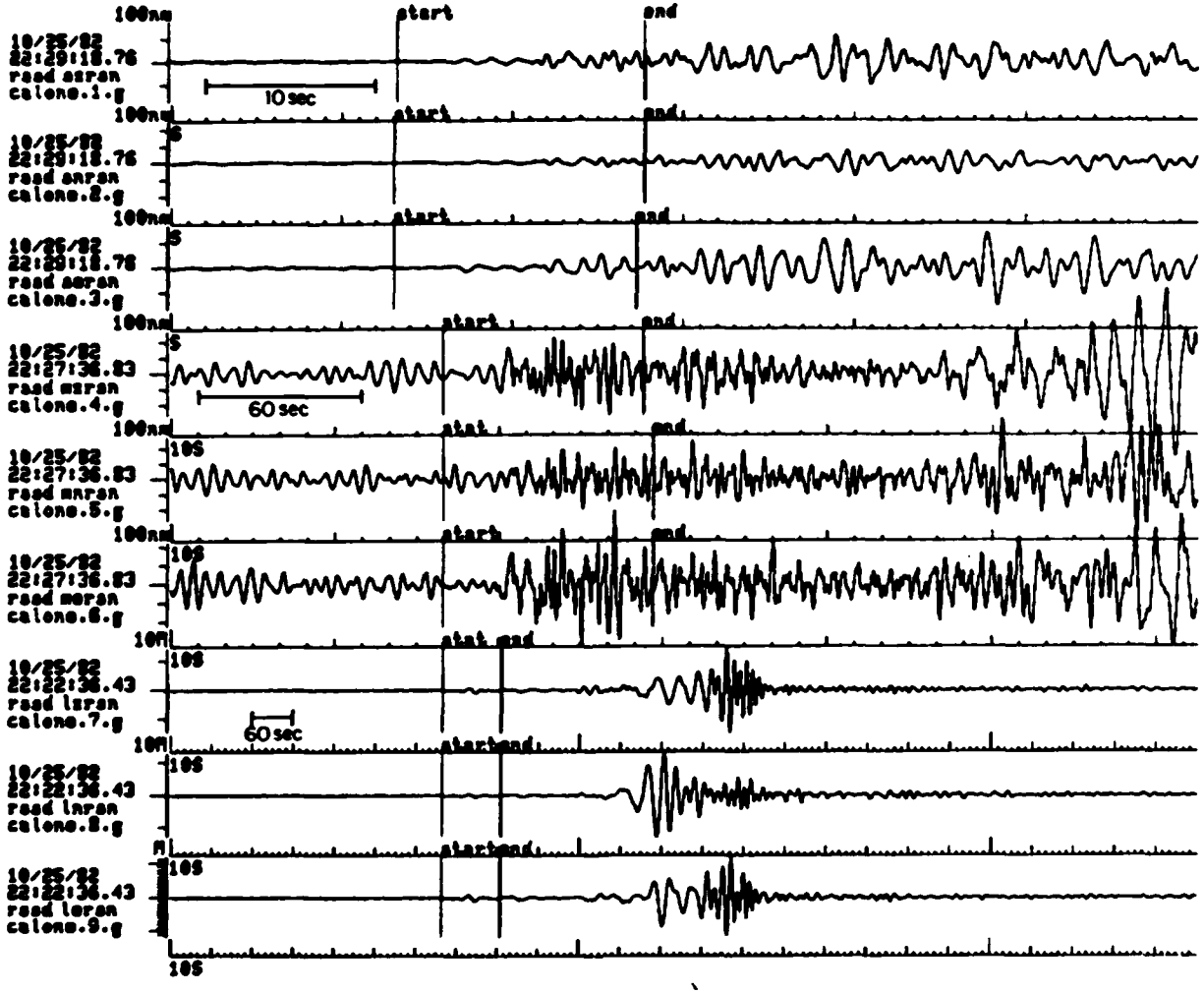

Figure 5A Calone-to-RSSD (14.78°) (Scales same as Figure 3) P wave, Love and Rayleigh surface waves are the long period records.

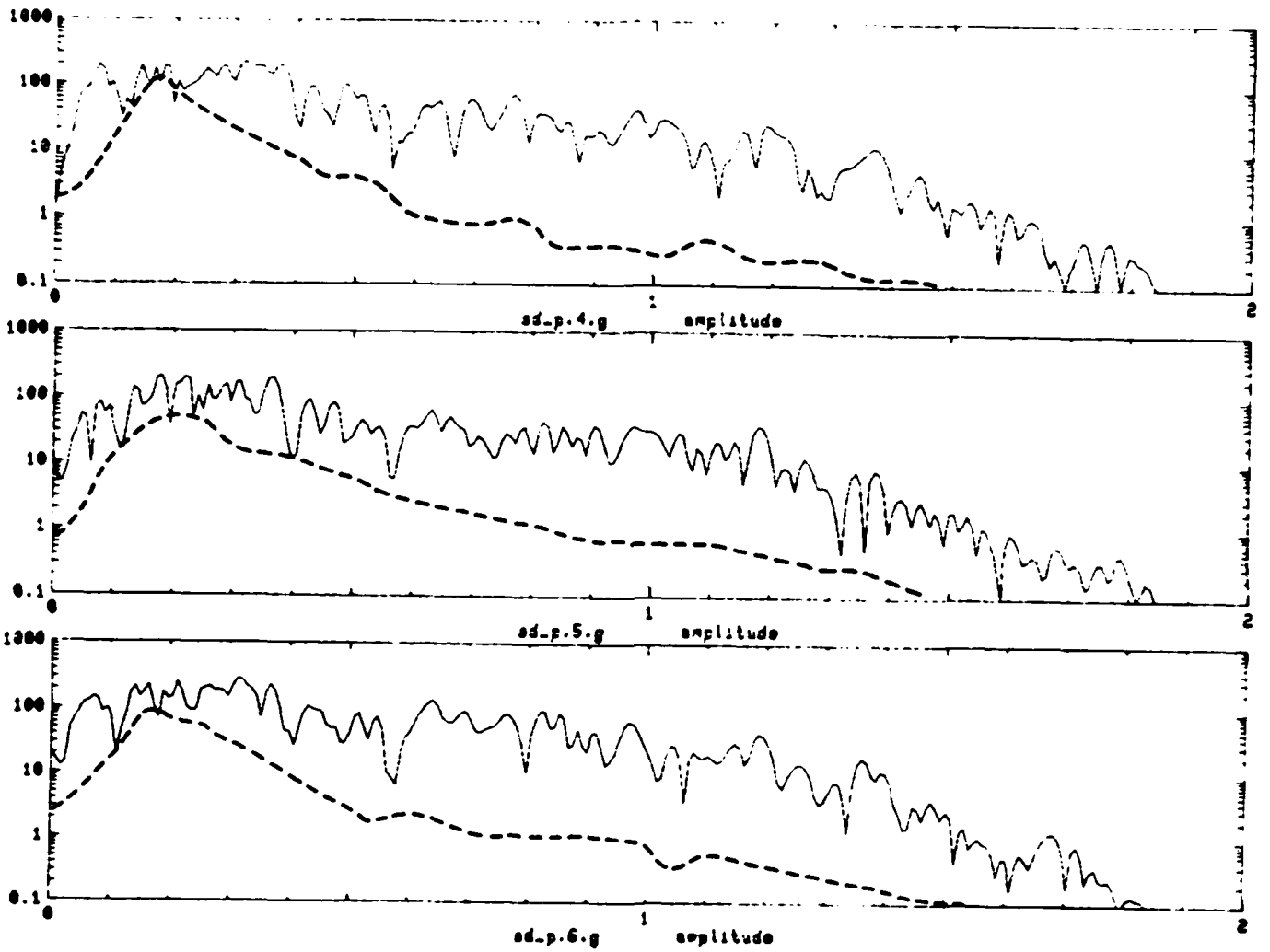

Figure 5B Calone-to-RSSD (14.78°) Mid period P wave amplitude spectra with noise estimates. P wave spectra remain above the noise across the microseism band at 0.2 Hz.

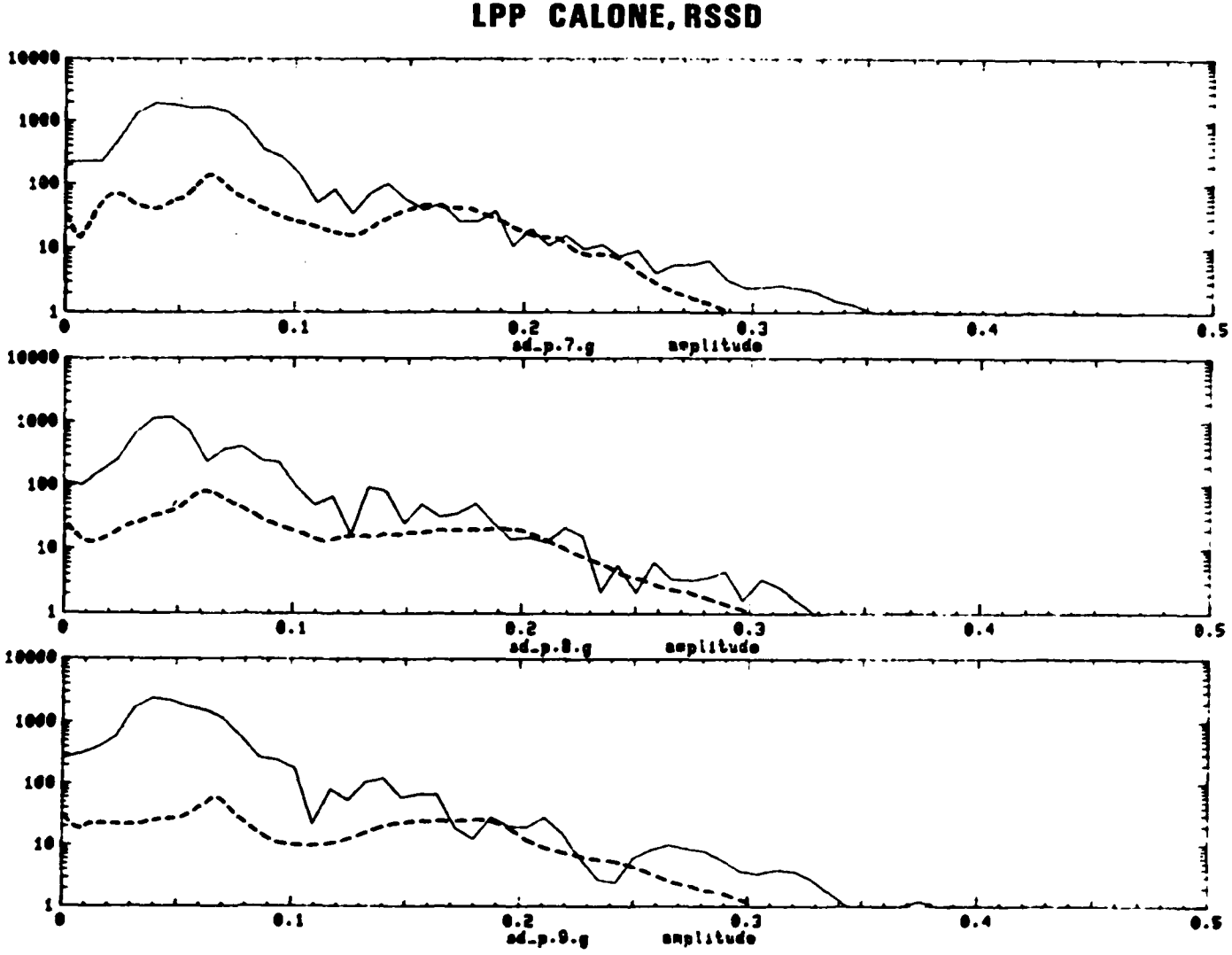

Figure 5C Calone-to-RSSD (14.78°) Long period P wave amplitude spectra with noise estimates. P wave spectra remain above the noise at frequencies below 0.1 Hz.

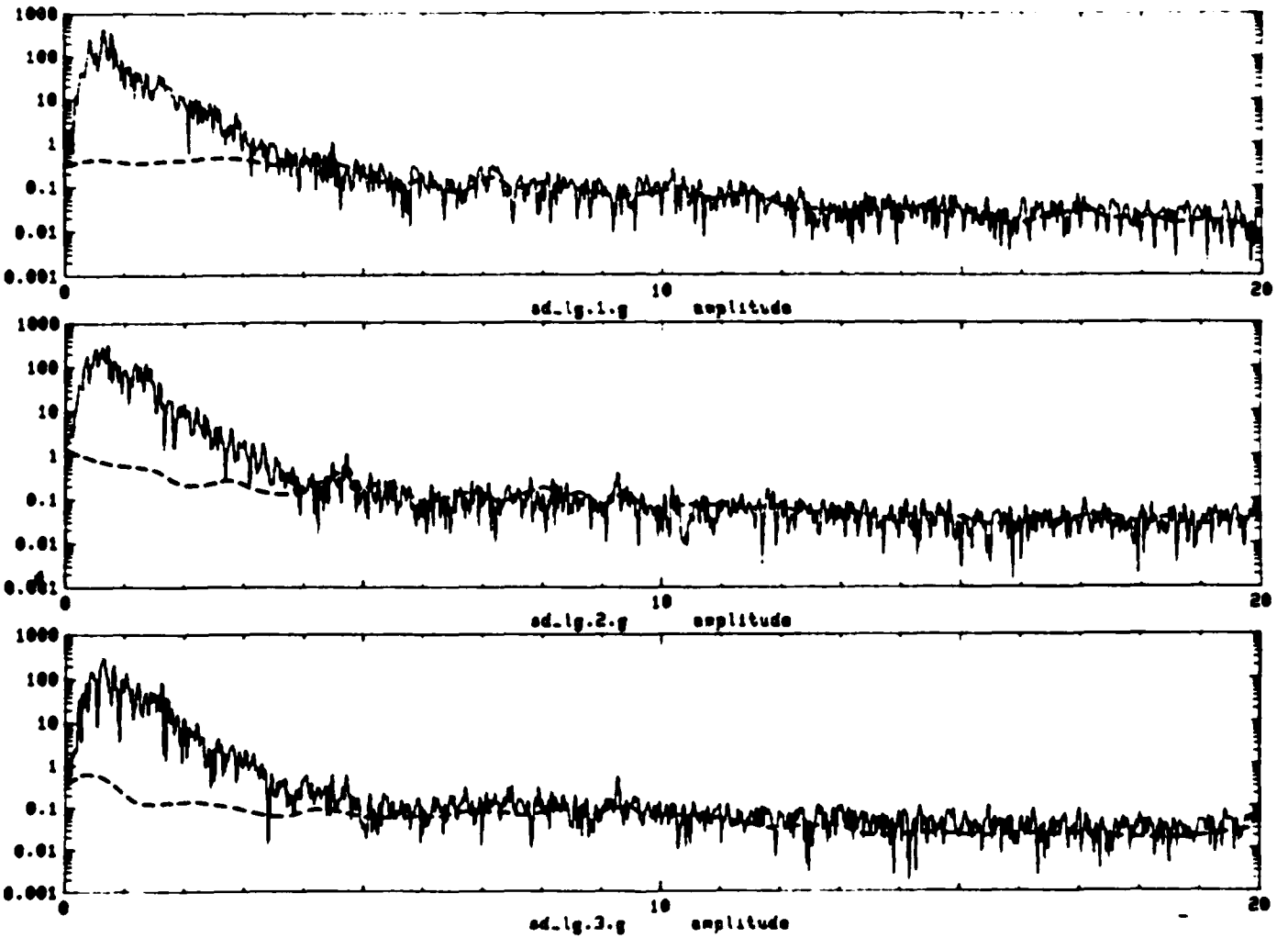

Figure 6A NTS-to-RSSD (11.49°) Short period Lg amplitude spectra with noise estimates. Signal strength is much the same on all three-components. Signal and noise amplitudes are flat at levels near .01 mu above 5 Hz. Maximum S/N estimates for Z, N, and E are 500, 285, and 250 at 0.7, 0.7, and 1.3 Hz respectively.

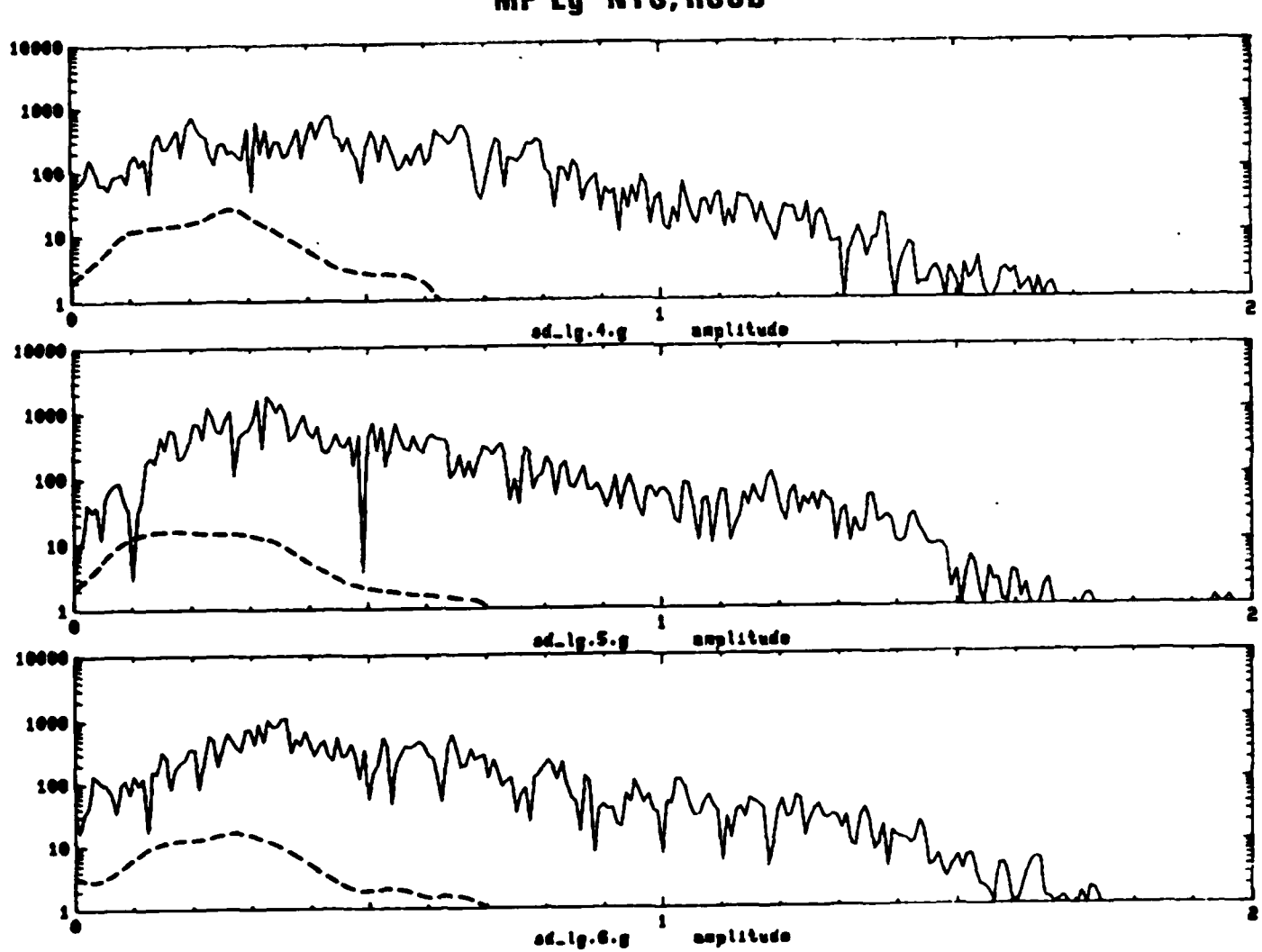

Figure 6B NTS-to-RSSD (11.49°) Mid period Lg amplitude spectra with noise estimates. Maximum signal-to-noise ratios at 511, 200, and 200 at 0.64 0.55 and 0.66 Hz. Lg signal is strong across the microseism band at 0.2-0.3 Hz.

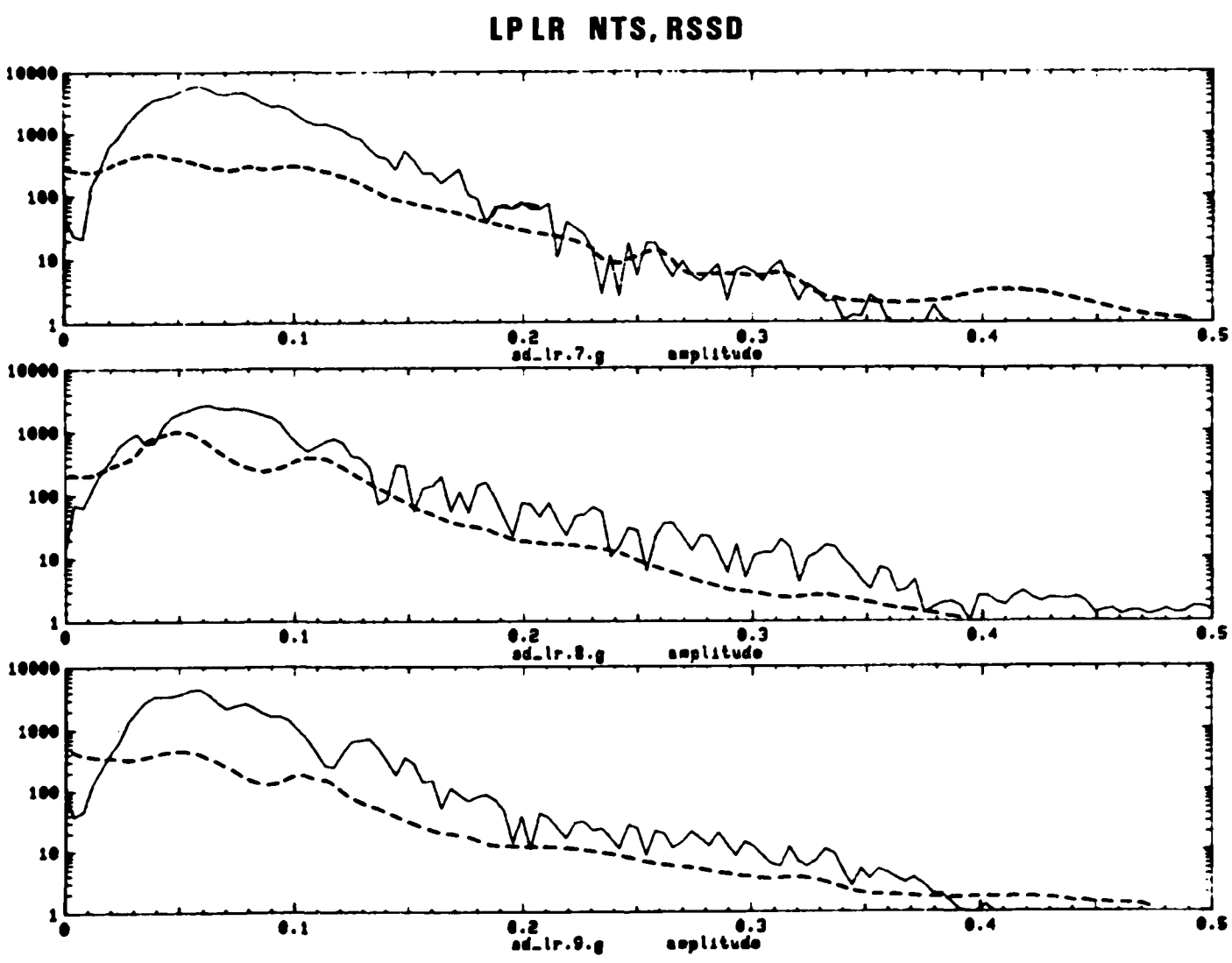

Figure 7 NTS-to-RSSD (11.49°) Long period L_R amplitude spectra with noise.

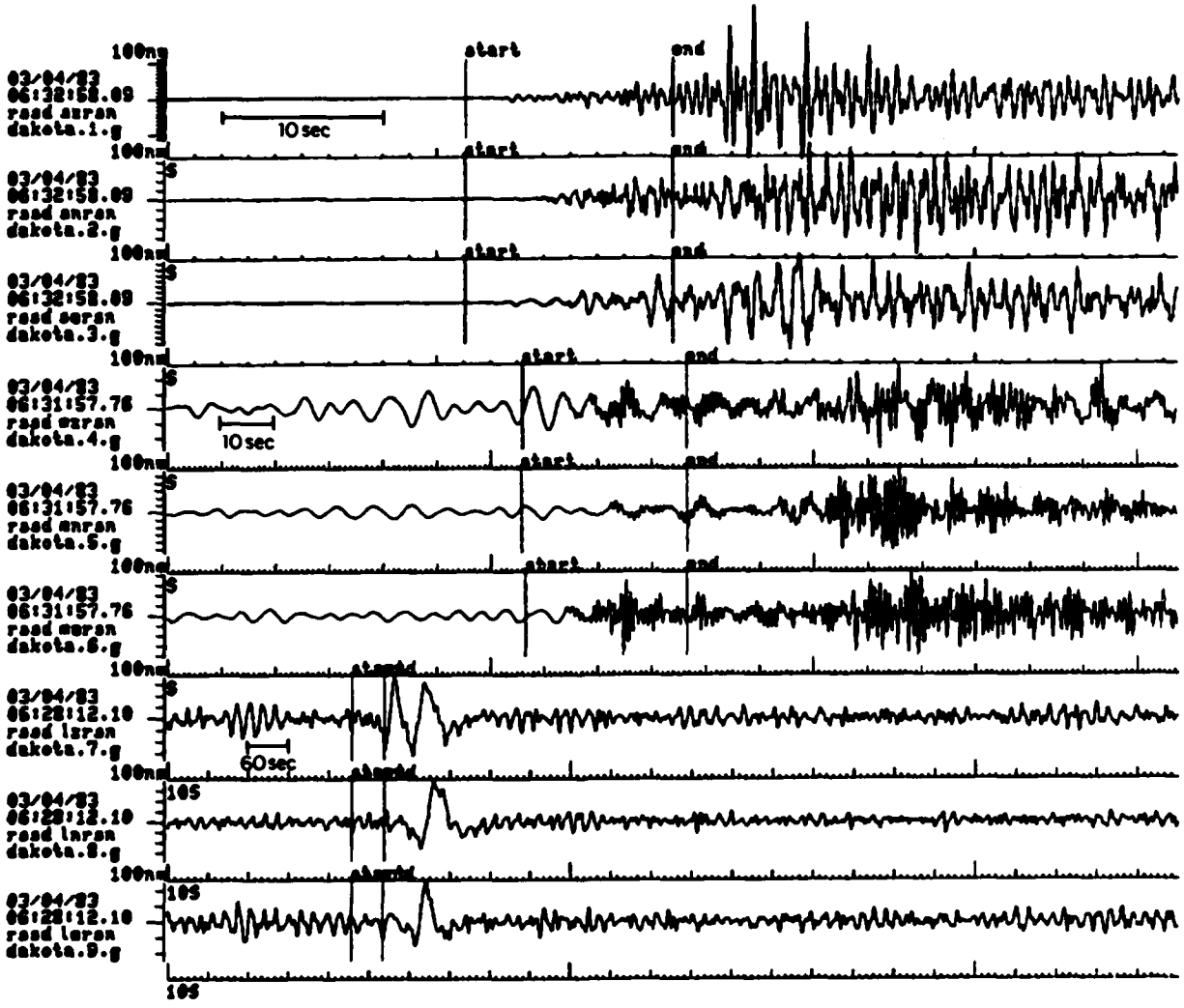

Figure 8 Dakota-to-RSSD (3.3°, M_L 4.4) Near regional event shows well developed P_n-Pg separation of 8 seconds on short period and mid period Z&E. (Azimuth of approach ESE) S waves and Lg are well developed on the mid period band. A Rayleigh pulse is prominent on the long period band.

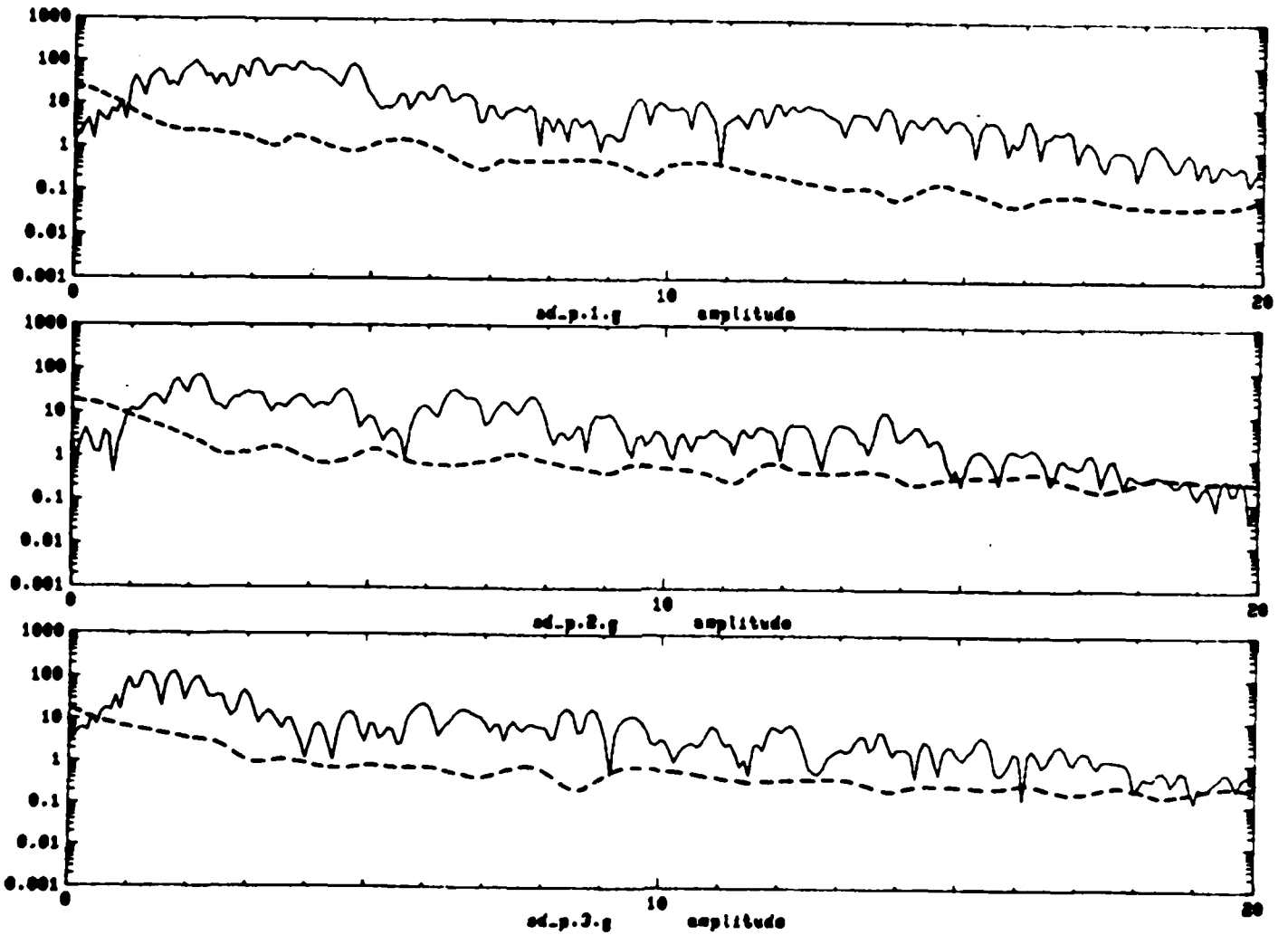

Figure 9A Dakota-to-RSSD (3.3°, M_L 4.4) Short period P wave amplitude spectra with noise levels. P wave spectra above the noise throughout the band width. Signal to noise has multiple local maxima at 3.7 and 13.1 Hz. (Noise estimate is plotted 1 decade too high)

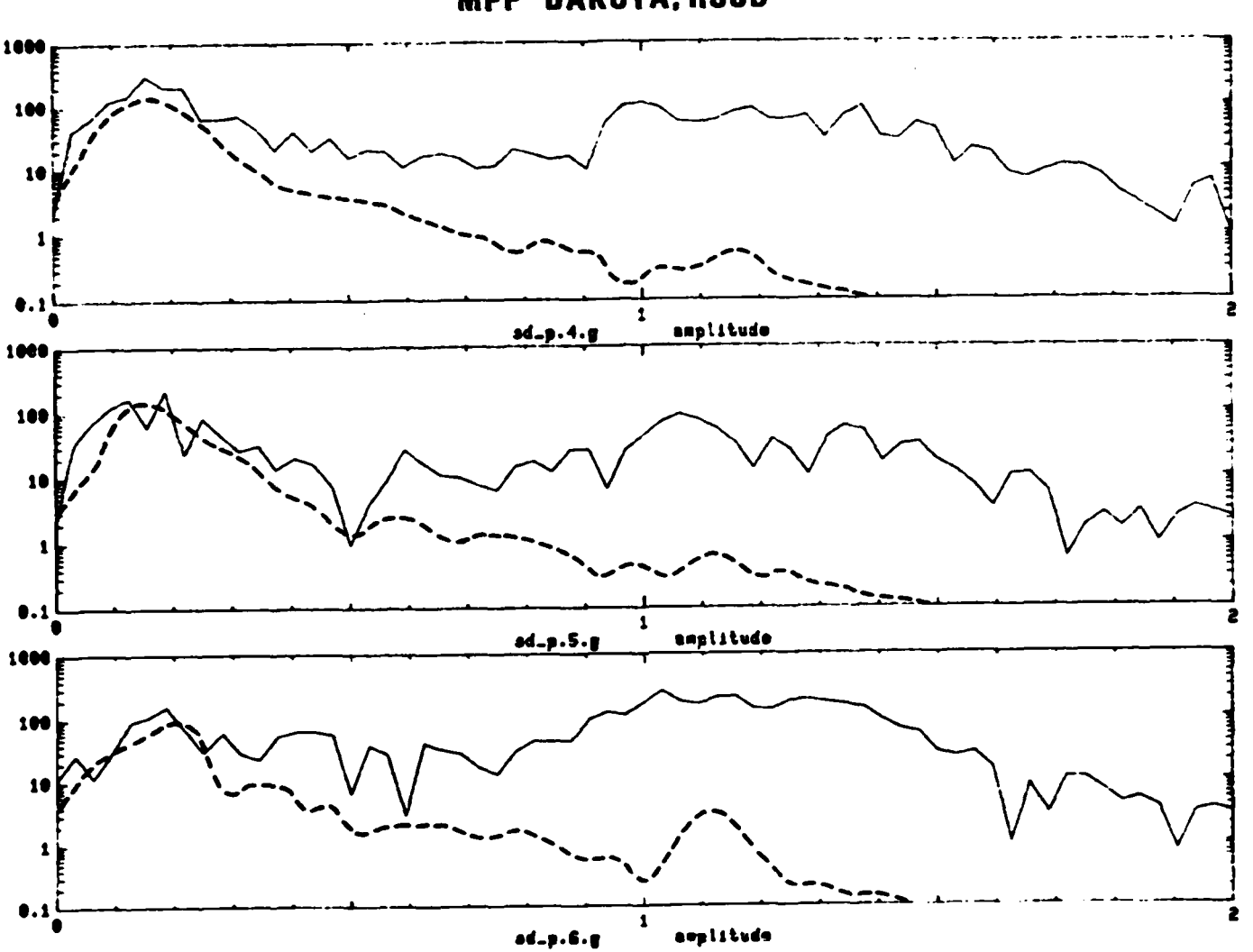

Figure 9B Dakota-to-RSSD (3.3°, M_L 4.4) Mid period P amplitude spectra with maximum signal-to-noise near 3 Hz.

signal level of ±.5 least significant bit (LSB), the quantization level. For the short period band, this corresponds to .01 mμ/$\sqrt{\text{Hz}}$ at the reference frequency of 1.0 Hz. At highest gain, the short-period LSB = 0.031 mμ and the effect of quantization noise may be viewed as white noise with rms amplitude of LSB/$\sqrt{12}$ (Openheim and Schafer, 1975) or 0.01 mμ. At the next lowest gain level the quantization noise level is .07 mμ. For a larger amplitude signal that was predominately recorded at a greater gain level, the quantization noise level will be higher.

Table III summarizes the short-period quantization noise levels at the four gain levels that are used with the automatic gain-ranging. To be precise, the white noise level contribution to the final spectra is a sum of the proportional time periods at each automatic gain level.

The limiting white noise level is at best .01 mμ at 1 Hz. When corrected for instrument response this means that some RSTN short-period recordings are sensing quantization noise and not local ground motion at frequencies above 10 Hz, during quiet time periods (Figure 6a noise levels). Furthermore, the flat signal spectra above their "noise" levels at high frequencies may not be significant since the signals were recorded at a higher gain levels than the ambient "noise" signals. Consequently, it is not clear that the signals observed in Figures 4a, 6a and 9a are at or below ambient noise levels at high frequencies. Previous studies of ambient noise levels at quiet sites (Herrin, 1982; Fix, 1972) indicate that ambient noise levels continue to decline at high frequencies.

The frequency response and gain levels of the RSTN instruments were designed so that the expected ambient ground noise averaged over 1/2 octave bands, was an rms 5 counts up to 10 Hz. The response declines at frequencies above 10 Hz to ensure that aliasing of ground and system noise is unimportant. The model for ambient ground noise was based on known quiet sites such as Lajitas (Herrin, 1982). Recent reports from NORSAR (Bungum, 1983) indicate that southeastern Norway has very similar noise levels at 10 Hz. If these are globally representative noise levels then it is expected that such quiet sites as RSSD will show quantization noise from time to time for frequencies near and above 10 Hz. This is not unexpected given the design criteria of the RSTN response.

TABLE III

Short-period Band Quantization White Noise Contribution at Different Gain Levels.

Gain Level Indicator	Resolution LSB $m\mu$	RMS White Noise Level $m\mu$
11	3.99	1.15
10	.99	.28
01	.25	.07
00	.031	.01

Estimation of Detection Thresholds

An effort was made to estimate detection thresholds as a function of distance for P, Lg and L_R within the three frequency bands. Figure 10 illustrates the procedure using the NTS (M_L 5.4) event and short period, P-wave and Lg signal-to-noise estimates. The location of the NTS event is shown together with the five RSTN stations. At each station the logarithm (base 10) of the maximum signal-to-noise ratio is shown and the frequency at which it was measured. In the case of RSNY the short period Lg was not detected. In the case of RSCP, the Lg record was not available. The difference between the log(S/N) and the local magnitude provides an estimate of the possible detection threshold. For instance, an estimate of M_L 3.0 is derived for the detection threshold at RSSD for the NTS source area on the short period instrument. A value closer to 5.0 M_L would be indicated for short period Lg. Similarly, Figure 11 presents the short period and long period P-wave signal-to-noise ratios, (S/N), for the Dakota earthquake. Figures 12 and 13 show the (S/N) for the Arkansas and New York earthquakes.

The M_L was used in these analysis where available since it more properly measures the high frequency content of the source than the low frequency measure M_S or the narrow band measure m_b. Because the velocity response of the middle and short-period band recording is flat in the pass bands of interest, the amplitude measurements were not corrected to period; (A) not (A/T) was used in the analysis.

All the estimated short-period detection thresholds are combined in Figure 14 and plotted versus distance. Each estimate is coded acording to event number. If no short period P detection was made an up arrow (↑) indicates the lower limit that is implied by the lack of detection.

The intra-shield paths of events (3) Arkansas, (4) Yellowstone, (6) Gaspe, (7) New York, and (9) South Dakota may have systematically lower thresholds. The non intra-shield paths of (5) NTS, (2) and (5) California, and (8) Mexico could be expected to pose additional attenuation to P-waves. Some of the Lg (S/N) is presented in Figures 15, 16, 17, and 18 together with the L_R (S/N) data. The Lg detection

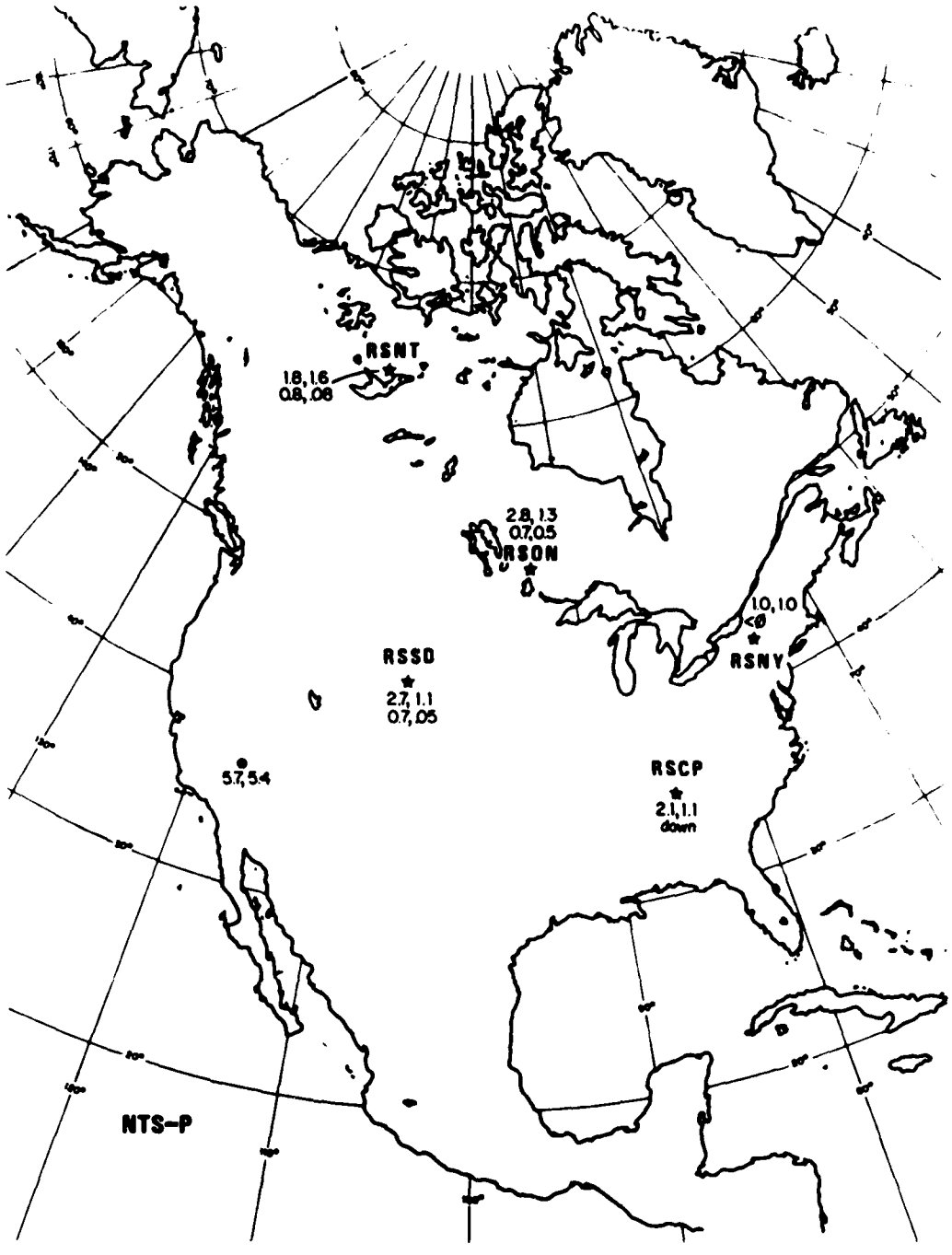

Figure 10 NTS short and long period P wave detection: P logarithmic maximum signal-to-noise ratios and frequency at which the maximum signal-to-noise was measured. The top pair of values is for short period P and the bottom pair of values is for long period P. The M_L 5.7 NTS explosion had a P wave logarithmic signal-to-noise ratio of 2.7 at 1.1 Hz RSSD (3.3°). Similarly the long period P logarithmic signal-to-noise ratio was 0.7 at 0.34 Hz. A detection threshold of M_L 3.0 for this path is indicated for P and M_L 5.0 for long period P.

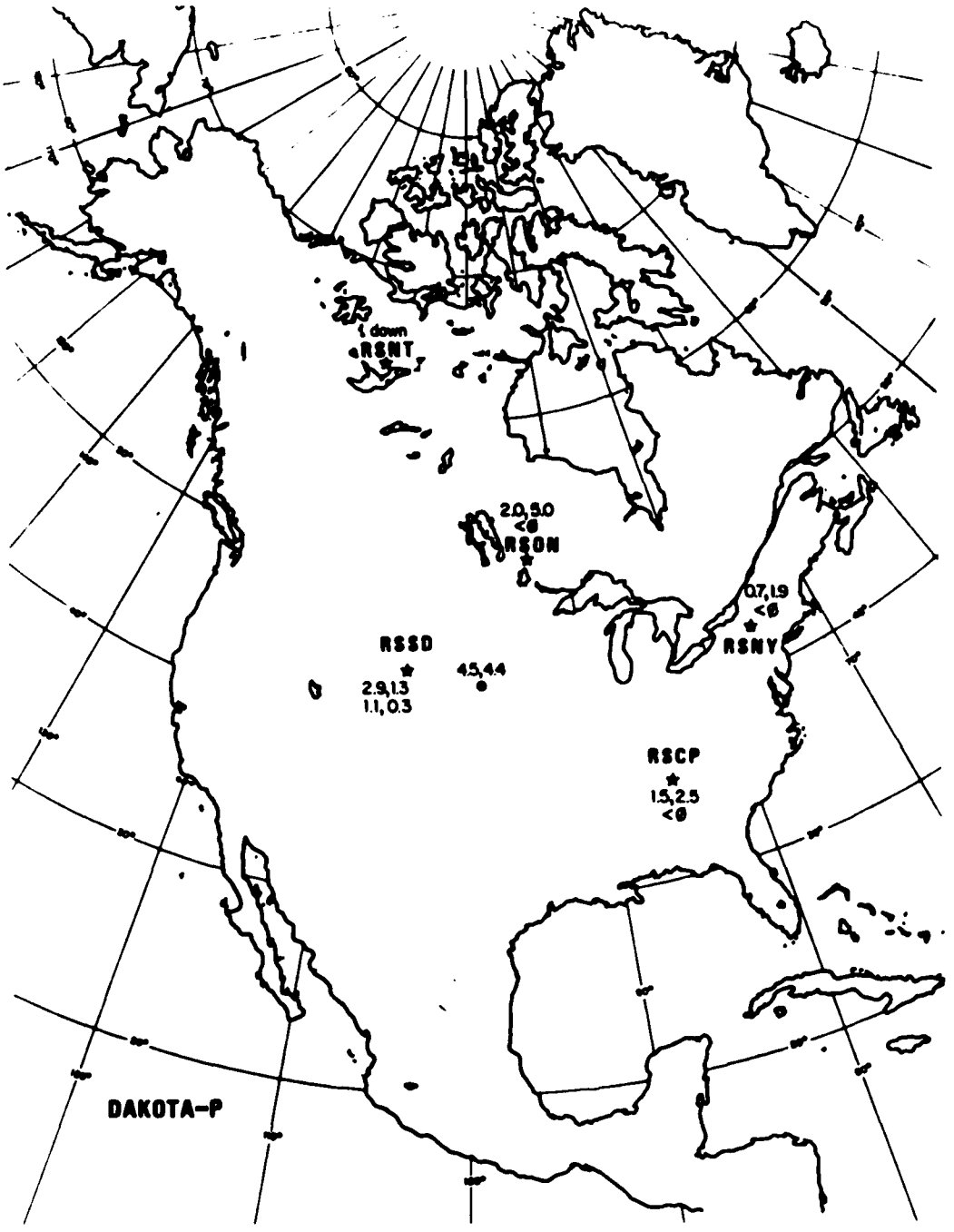

Figure 11 Dakota earthquake (M_L 4.5) short period and long period P wave detection. RSNT records were not available for this event, and long period records did not show a P wave for this event at RSON, RSNY and RSCP (< 0). A logarithmic P wave signal-to-noise ratios of 0.7 at RSNY indicates that a detection threshold of 3.8 or better is possible for intra-shield distances of 17°. Similarly a detection threshold of 2.5 may be indicated for RSON at 8°.

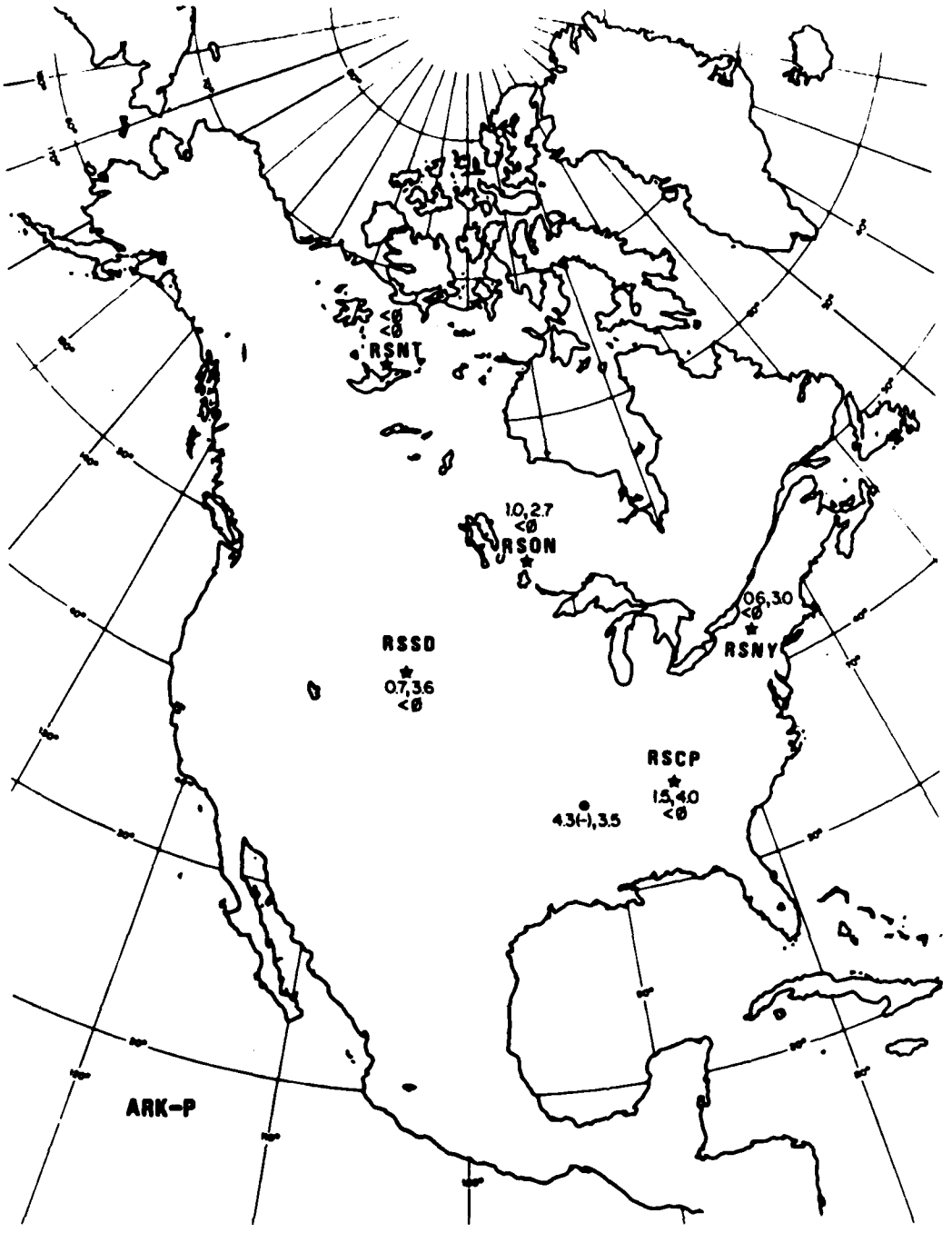

Figure 12 Arkansas earthquake (M_L 3.5) Short and long period P wave detection and logarithmic signal-to-noise ratios. The event was below detection threshold at RSNT for both short and long period P waves and below long period threshold for all stations. Short period detection threshold of 3.8, 3.7 and 3.3 are indicated for the path to RSCP (5.4°), RSNY (16°) and RSON (16°) paths.

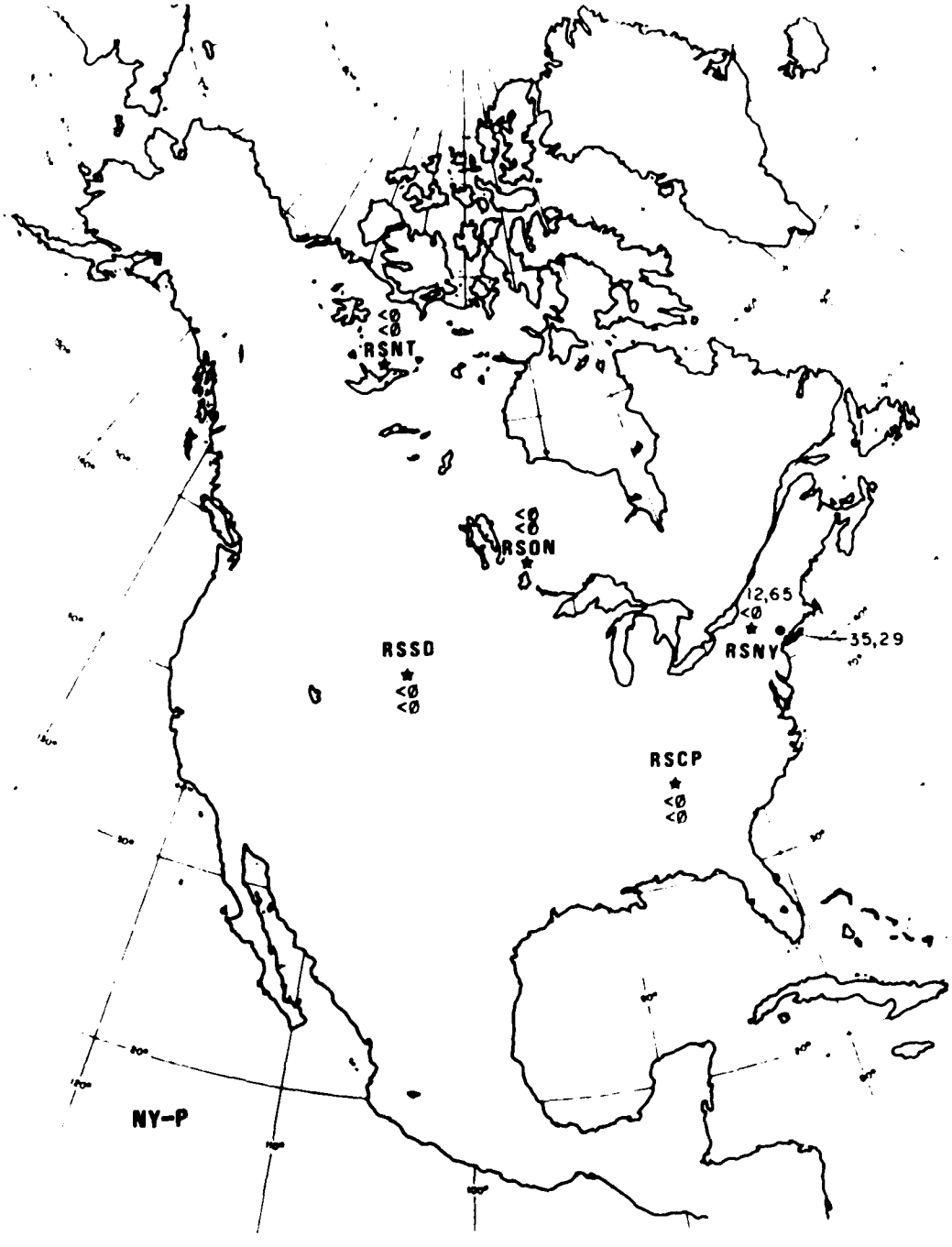

Figure 13 New York earthquake (M_L 2.9) short and long period P wave detections.

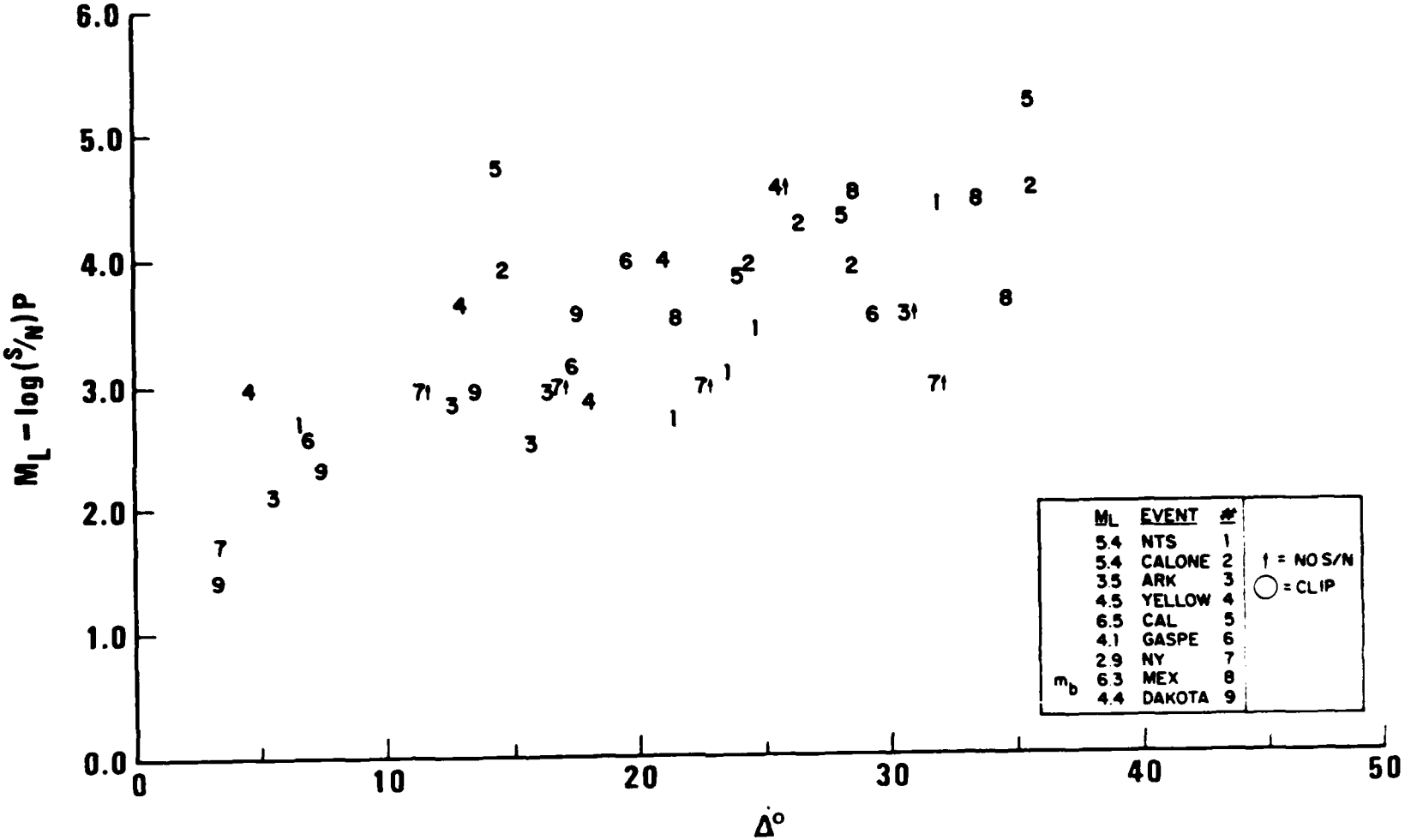

Figure 14 Estimated detection thresholds from short period P signal-to-noise ratios. No short period P detections are indicated by †. Non intra-shield paths NTS (5), Calone (2), CAL (5) and MEX (8) may be systematically higher than intra-shield paths ARK (3), Yellow (4), GASPE (6), NY (7) and Dakota (9).

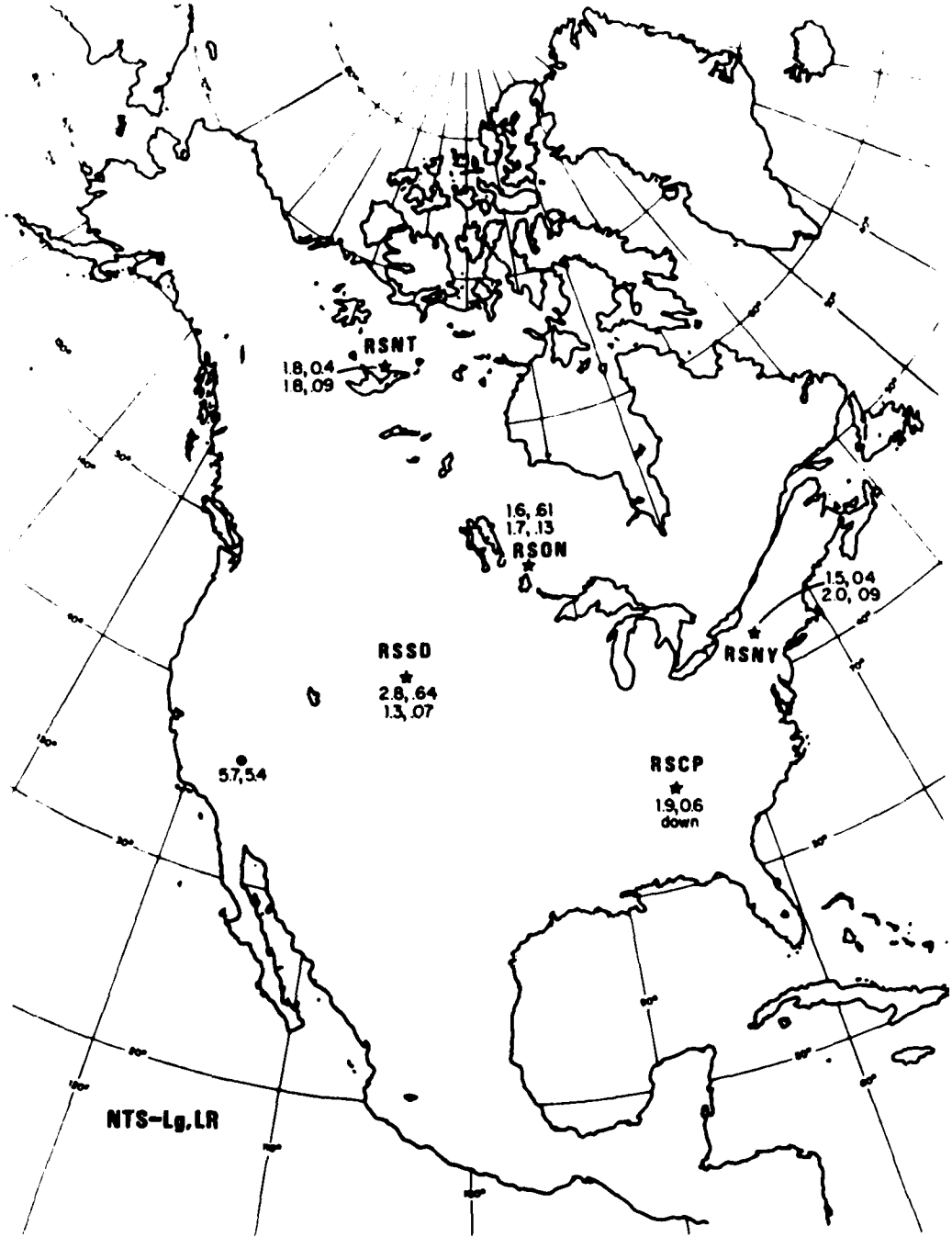

Figure 15 NTS explosion Lg and L_R logarithmic signal-to-noise ratios. Top pair is logarithmic S/N and frequency for Lg. Bottom pair is for L_R.

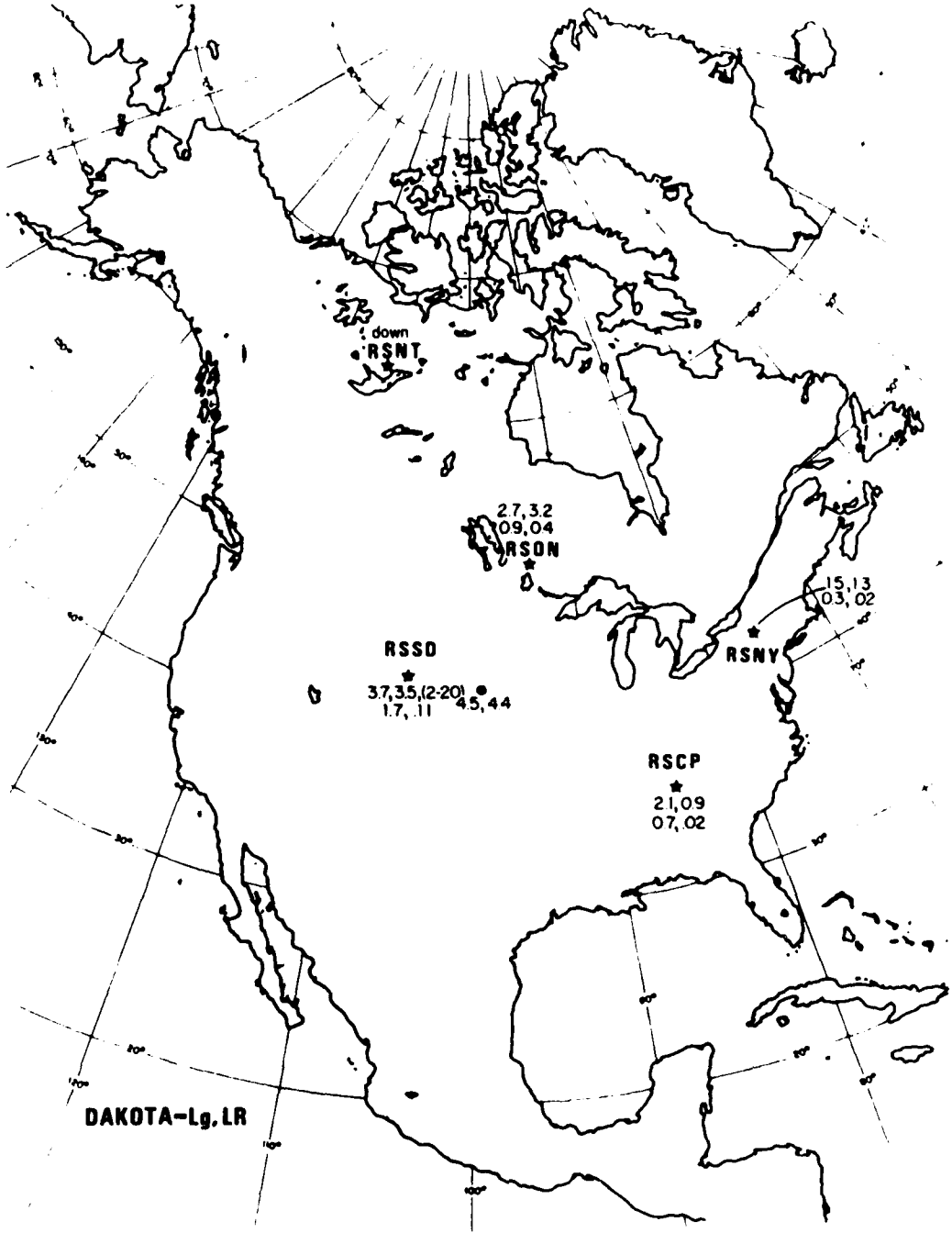

Figure 16 Dakota earthquake Lg and L_R logarithmic signal-to-noise ratios earthquake.

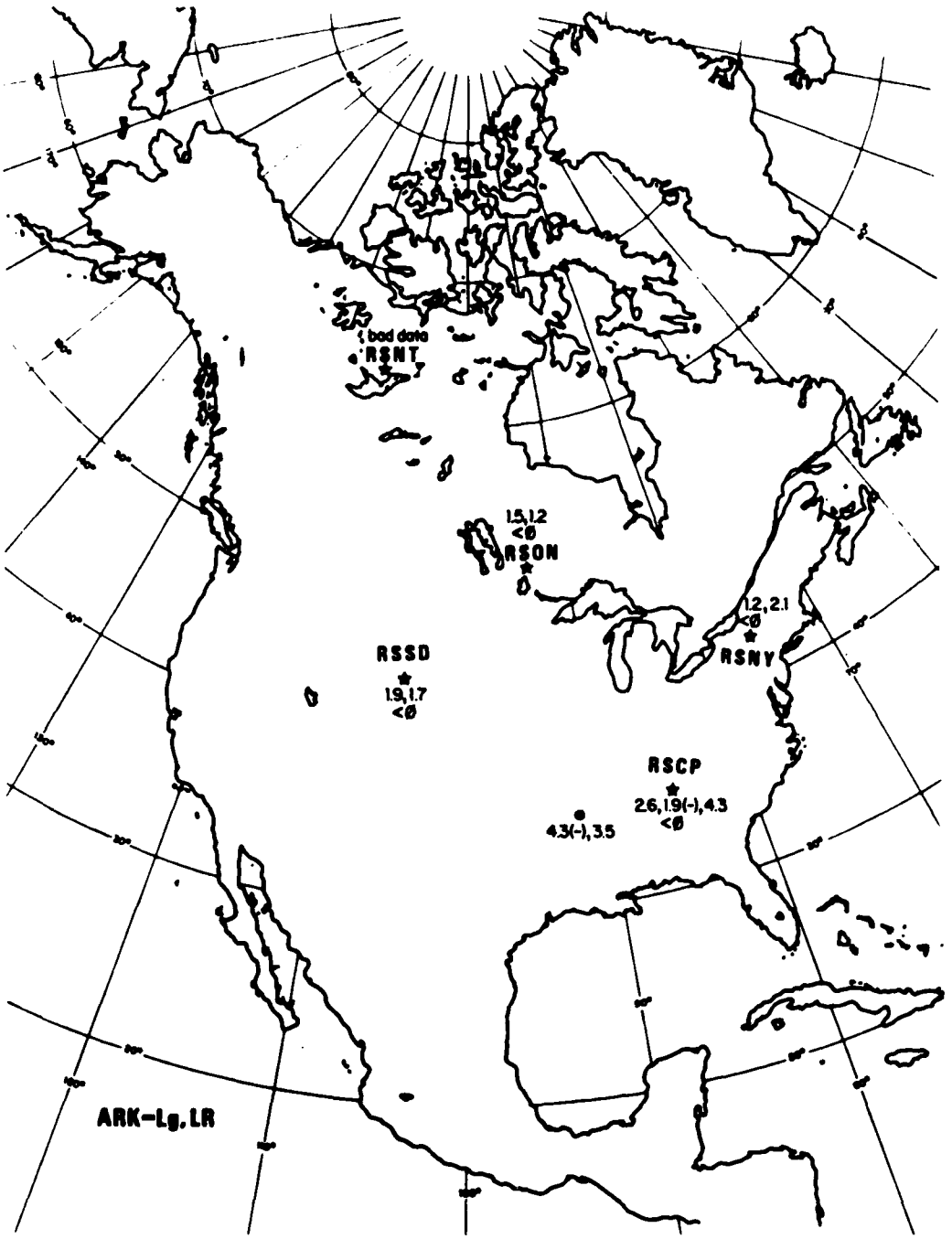

Figure 17 Arkansas earthquake Lg and L_R logarithmic signal-to-noise ratios.

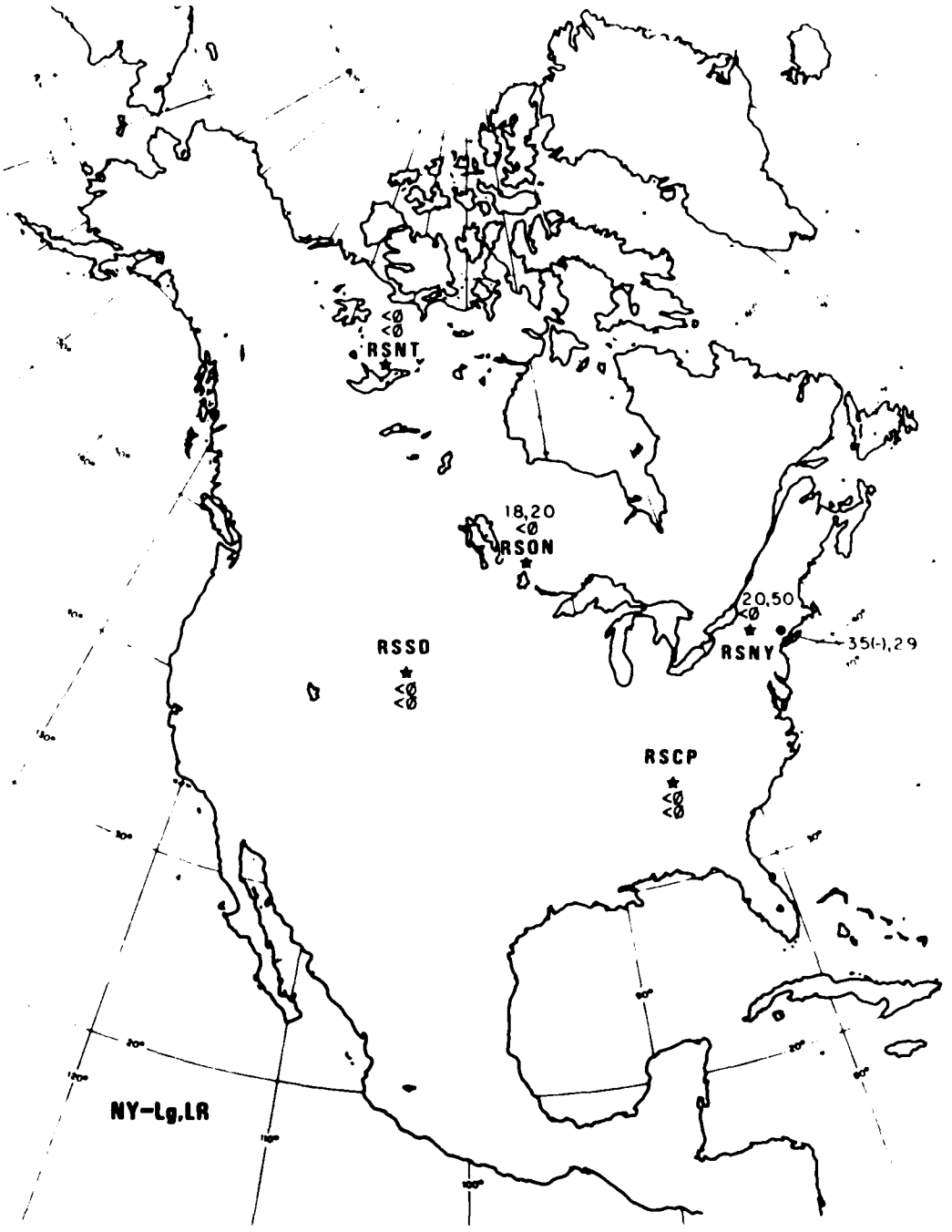

Figure 18 New York earthquake Lg and L_R logarithmic signal-to-noise ratios.

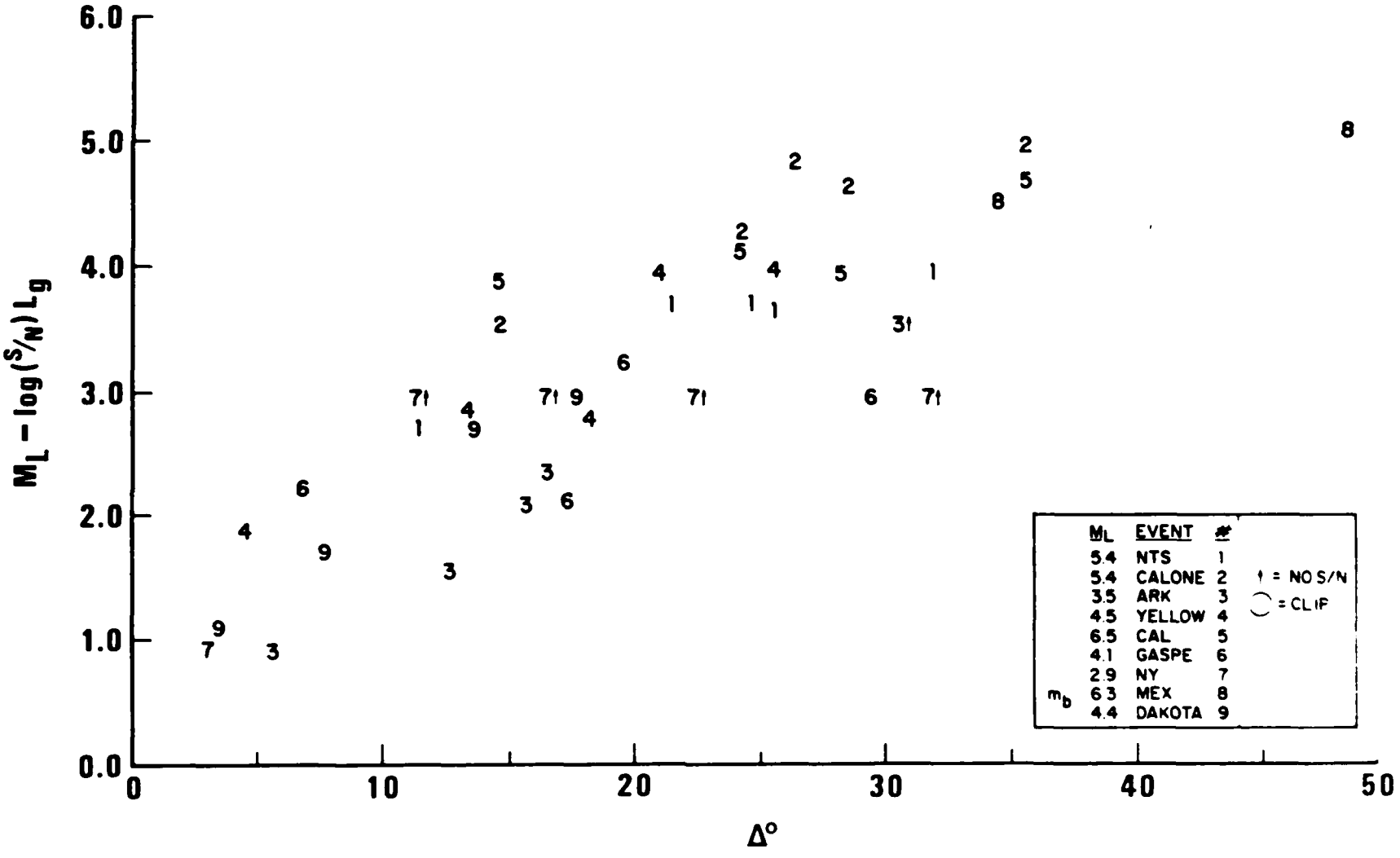

Figure 19 Lg detection threshold versus distance for the nine studied events. Lg detection thresholds are not significantly below P wave detection thresholds of Figure 14.

estimates are gathered in Figure 19 as a function of distance. The estimated Lg detection thresholds are significantly better than the estimated P-wave detection thresholds of Figure 14 for distances greater than 15 degrees. This may be an artifact that events from the tectonic provinces of North America dominate the longer paths sampled, and the larger magnitude events.

L_R detection thresholds derived from (S/N) estimates are compiled in Figure 20. The $r^{-1/2}$ curve is plotted for comparison. The large (m_b 6.3) Mexican earthquake may yield a biased estimate of the L_R detection threshold because of source scaling effects. Larger events, with corner frequencies below 1 Hz, are not adequately characterized by the 1 Hz m_b estimate. Since the m_b estimate for such an event is probably an under estimate of the low frequency L_R generated by the event, the L_R thresholds for (8), the Mexican earthquake, are biased low.

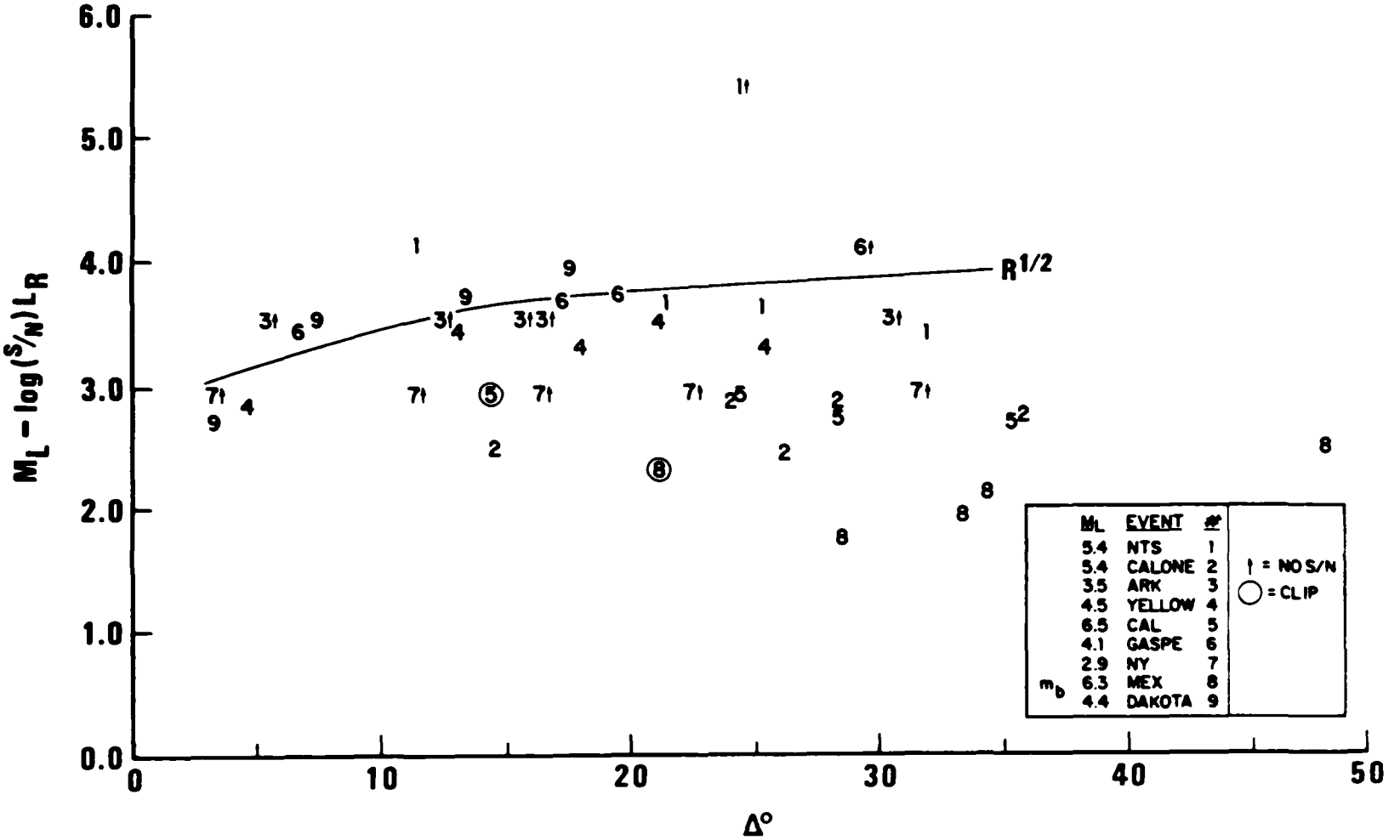

Figure 20 L_R detection thresholds versus distance derived from signal-to-noise ratios. 0's indicate clipping of signal and consequently biased estimates of detection threshold.

Data Flow at the CSS

Tapes of the RSTN data in SCARS format were directly recorded at the CSS or were obtained from SCARS by request. It was found that existing software at the CSS did not properly identify and process calibration sequences. Furthermore, dead spots were found in the digital data recorded at the CSS. These data drop-outs were usually brief intervals of zeros (c.f. Figures 21a and 21b). To alleviate the problem of drop-outs and calibration sequences, some tapes were requested from SCARS to supplement the locally recorded data. The requested SCARS tapes had significantly fewer digital drop-outs, but the problem still persisted. The data drop-outs appear to be the result of variations in the satellite signal characteristics. A detection algorithm for these brief strings of zeros was added to the Transform program resident at the CSS.

The RSTN data was passed through two programs NSSREAD and NSSTODB to the INGRES data base management system. A shell script was developed to extract the RSTN digital data and associated calibration information to a local data base consisting of seismograms and directory information. Programs display, transform and spectrum could then be used to plot the waveforms, and calculate Fourier spectra of the digital waveforms on a Tektronix storage tube terminal. The plotting format options of spectrum were modified to accomadate the desired spectral plots. A serious "bug" in the program transform was discovered that resulted in severe aliasing of the resultant spectra. Corrections were made to the program transform and tapering options were added to the algorithm. The post detection arrival detector was found to be inadequate to the task of automatic detection. The algorithm stops with its first detection and could not be modified. Data drop-outs and noise bursts confused the algorithm, and produced too many false alarms. The algorithm could not adjust its detection criteria to a changing noise environment. Amplitudes and predominant periods of the seismic phases were measured with the disp program on the Seismic Analysis Station (SAS).

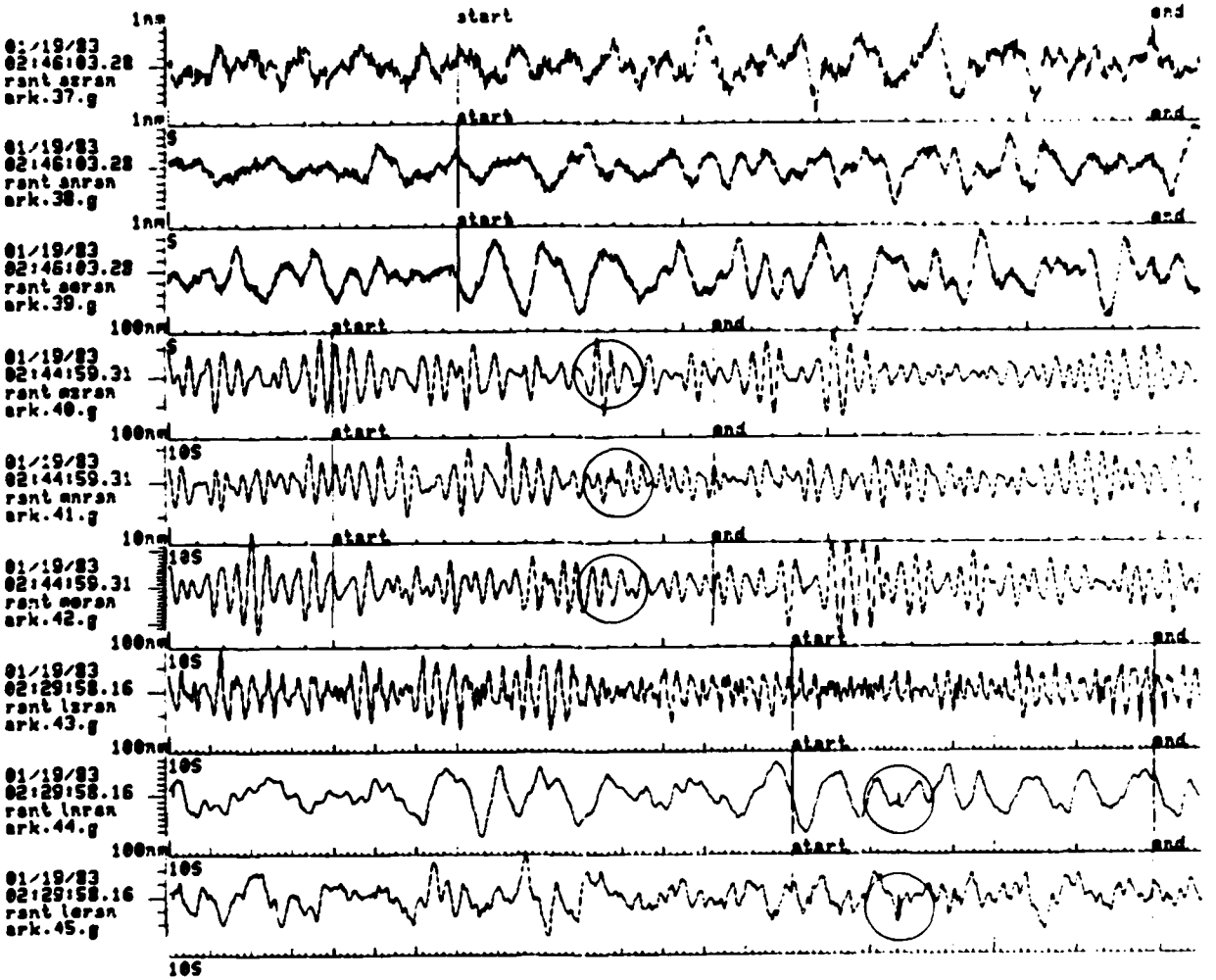

Figure 21A Example of data dropouts in middle and long period data.

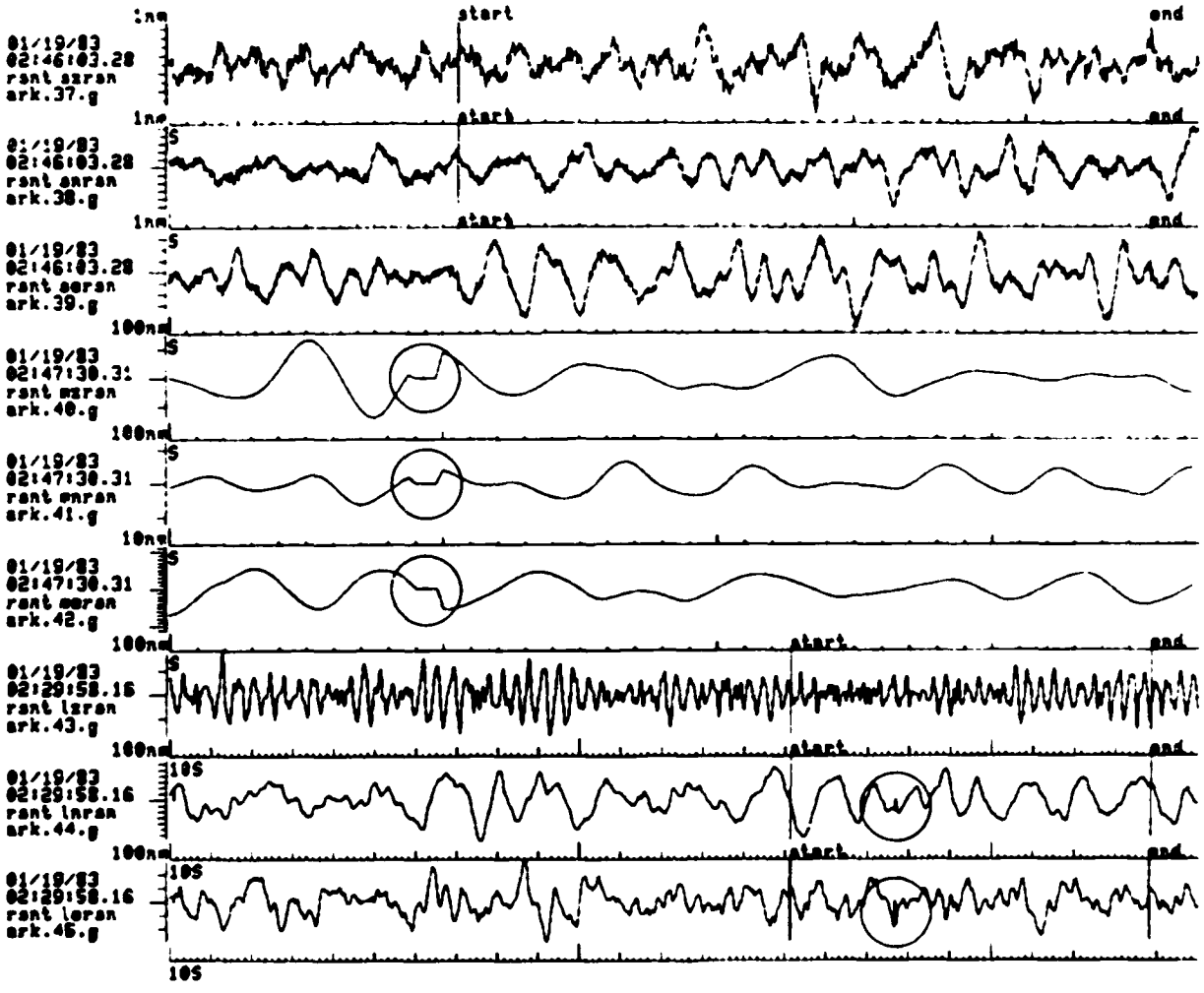

Figure 21B Expanded view of dropout of the middle period.

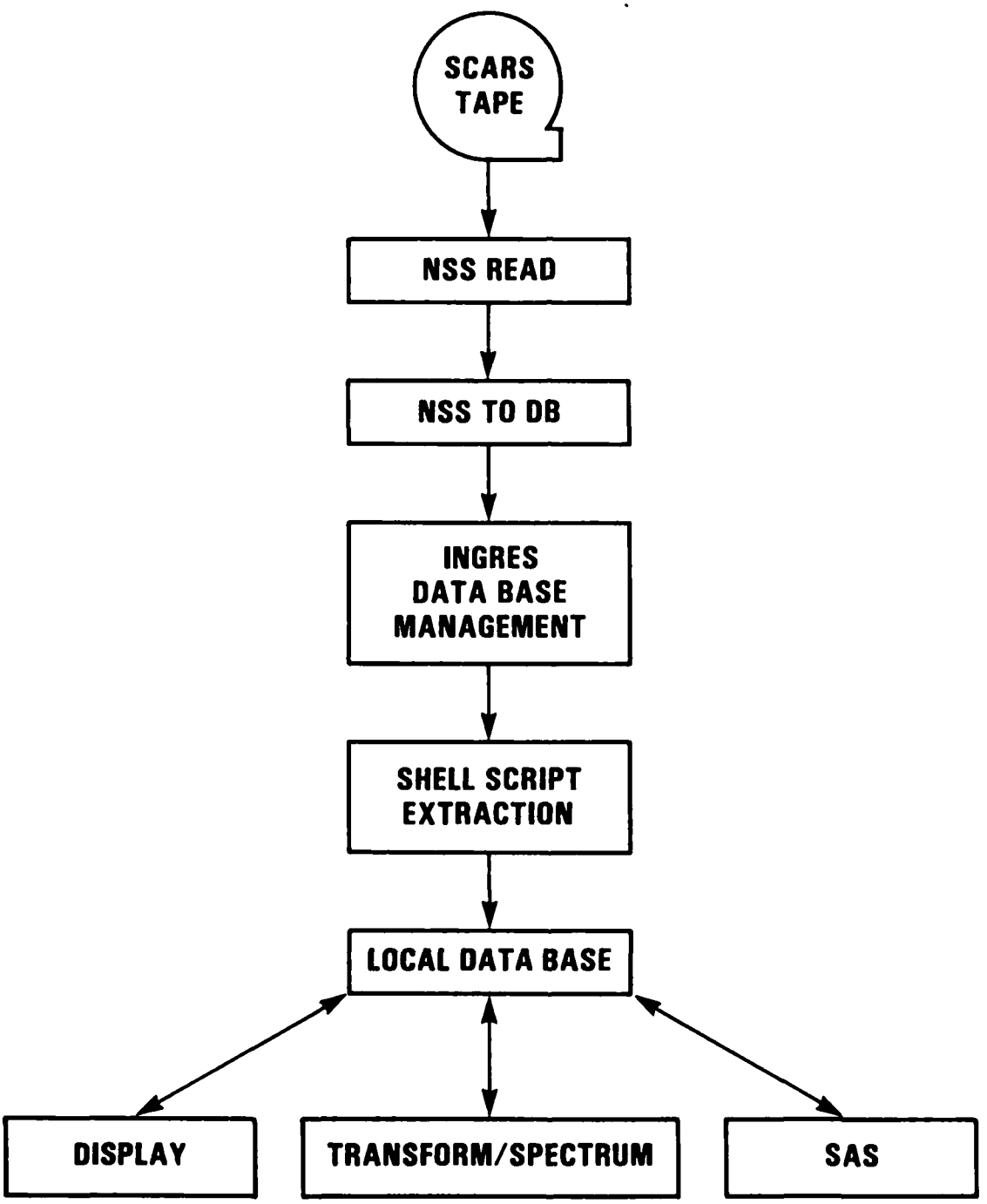

Figure 22 Data Flow at the CSS

FURTHER IMPROVEMENTS TO AUTOMATIC ASSOCIATION (AA)

Using the artificial data we had created for the International Data Exchange Exercise, we tested Automatic Association (AA) with the objectives of comparing its performance to Center for Seismic Studies (CSS) AA, and to develop and include some AA features used by the Swedish AA and the CSS AA not yet present in the Seismic Research Center's (SRC) AA. In addition, we developed and implemented the following features into SRC's AA.

- Kinematic/dynamic use of amplitude data
- two array event location
- use of pP and sP to attempt to automatically constrain depth
- slowness check on all phases (not just P and PKP)
- show unassociated arrivals in final summary bulletin
- include confidence ellipses in summary bulletin

A comparison of the two AA's from SRC and CSS has not been accomplished yet, mainly because the two AA programs were executing on different computers and a common mutually-readable data set has not been defined.

Documentation for AA was completed and printed in Seismic Research Information System (SRIS), (1982).

Kinematic/Dynamic Use of Amplitude

Theoretical basis for this work has been described in a memorandum by R. R. Blandford dated 7 October 1982 and a practical embodiment of the scheme is described in another memorandum by Blandford dated 19 April 1983. (Both memoranda are contained in Appendix II). An efficient Newton-Raphson procedure for computing the maximum likelihood magnitude (Ringdal, 1976) offers a computational improvement.

For a chosen network of stations, not necessarily the full network of detecting station, a maximum likelihood estimate of body wave magnitude m_b using the amplitudes of the locating arrivals. Clearly there are three special cases to consider regarding the network of "reliable" stations, the stations that actually detected, and the amplitudes of the detections.

1) A station does not report a detection even though the m_b indicates that it should have detected. 2) A station reports a detection and the m_b indicates that it should not have detected. 3) A station reports a detection but the amplitude is either too high or too low according to the m_b. Figure 23 shows the the numerical modification to the accumlated screen points for these three cases, and Figure 24 is an up to date list of the numerical values for the attributes considered in the SCREEN subroutine.

- SELECT "RELIABLE STATIONS", GET DETECTION THRESHOLDS

- COMPUTE RINGDAL M_B

- IF A STATION DID NOT DETECT BUT SHOULD HAVE, SUBTRACT POINTS, i.e.:

  IF $P(DET) > .95$: -1.0
  $P(DET) > .99$: -2.0

- IF A STATION DID DETECT AND REPORTS AN 'UNUSUAL' AMPLITUDE, A_0, DISCARD THAT AMPLITUDE FOR THIS EVENT,

  IF $P(AMP > A_0) < .01$ OR
  $P(AMP < A_0) < .01$ THEN REJECT A_0, START SCREEN OVER

- IF A STATION DID DETECT BUT SHOULD NOT HAVE, DISCARD ALL POINTS DUE TO THAT STATION, i.e.:

  IF $P(DET) < .01$, - (ALL POINTS DUE TO STATION)

Figure 23 Amplitude Modifications to SCREEN

AUTOMATIC DETECTION:	+ 0.82
IF (θ) AND $\Delta < 90^{o}$:	+ 1.02
IF (R) AND $\Delta < 7^{o}$:	+ 0.85
ANALYST - CERTIFIED DETECTIONS:	+ 0.98
IF (θ) AND $\Delta < 90^{o}$:	+ 1.18
IF (p) AND $\Delta < 90^{o}$:	+ 0.89
IF (R) AND $\Delta < 7^{o}$:	+ 1.10
IF IN SHADOW ZONE:	- 0.65
IF S PHASE:	+ 1.10
IF IN CODA:	- 0.20
IF SLOWNESS ERROR LARGE:	- 1.07
IF NO LATER PHASES	- 0.50

5 POINTS REQUIRED FOR DECLARATION

10 POINTS IN A-SEISMIC ZONE

Figure 24 SCREEN Points

Depth Constraint with pP and sP

Our experience with analyst-named phases indicates a tendency to name the teleseismic phase next arriving after P as pP. In fact, the next arriving phase may not be pP, but it may be sP, PcP or some unidentified phase. Restraining depth to the analyst's P-pP time during location convergence could lead to difficulties in correct event location and association of phases.

These considerations lead to the "soft" treatment of pP and sP named phases described here.

The list of P arrivals that is about to be input to the HYPO location program is examined in time order. The arrival queue is searched for a detection at the same station that is labeled pP or sP. If an sP is found the search terminates and the depth for P-sP is used as an input depth to HYPO. HYPO is not constrained to this depth, however. If no sP is found, the smallest P-pP time, if any are found, is used to establish the input depth to HYPO, again unrestrained to depth. The idea here is to try to improve the initial depth estimate of the HYPO solution.

The situation where the depth is actually constained by labeled pP or sP phases occurs as follows. When an event has been made and fully associated, its detections are examined to see if there is an sP phase, labeled as such by AA, which had also been labeled sP by the analyst. If one is found this P-sP depth is used to constrain HYPO and the event is run again. If no sP is found, the same algorithm is applied to P-pP depth, using the smallest P-pP time, if any. This algorithm works very well with the artificial data because analyst labeled "sP" is always true in this data set. More work has to be done on this algorithm to expand its usefulness to real data.

Other AA Improvements

In addition to the two major improvements described above some continuing enhancements to AA were accomplished. The slowness check has been extended to include all phases recognized by AA. Previously the slowness check was limited to P and PKP phases during the location phase. Since the travel times for the remaining phases are computed by polynomial evaluation rather than by table lookup, this necessitated the creation of a complete, new program component in which there is duplication of several of the computational modules used in travel time determinations during location.

Two array station trial epicenters have been added, based on the intersection of their respective confidence ellipses. SRC's AA uses this as the last pass through the signal queue, so in general, very few events are started this way. It has been added to be compatible with other AA programs. Equations for the two array computation are shown in Figure 25.

Confidence ellipse information has been added to the summary bulletin in accordance with standard practice.

The format of the summary bulletin has been expanded so that "left-over" or unassociated detections are printed in-line with the events and their association. This printing is a great help in reviewing the bulletin and the performance of AA. Various printing highlights are used to make the unassociated detections differentiate from the associated detections.

$$\text{ARRAY 1}\begin{cases} \delta P_X^1 = \frac{\partial P_X^1}{\partial \theta}\, d\theta + \frac{\partial P_X^1}{\partial \psi}\, d\psi + \frac{\partial P_X^1}{\partial h}\, dh \\ \delta P_Y^1 = \frac{\partial P_Y^1}{\partial \theta}\, \delta\theta + \ldots \\ \delta T^1 = \frac{\partial T^1}{\partial \theta}\, \delta\theta + \ldots + \delta T_0 \end{cases}$$

$$\text{ARRAY 2}\begin{cases} \delta P_X^2 = \frac{\partial P_X^2}{\partial \theta}\, \delta\theta + \ldots \\ \delta P_Y^2 = \frac{\partial P_Y^2}{\partial \theta}\, \delta\theta + \ldots \\ \delta T^2 = \frac{\partial T^2}{\partial \theta}\, \delta\theta + \ldots + \delta T_0 \end{cases}$$

OR

$$\underline{\delta} = B\underline{dx}$$

$$\underline{dx} = (B^T \Sigma^{-1} B)^{-1} B^T \Sigma^{-1} \underline{\delta}$$

Σ CONTAINS TRAVEL TIME AND SLOWNESS ERROR VARIANCE ESTIMATES DOWN THE DIAGONAL

Figure 25 Two-Array Location

Future Improvements

As mentioned earlier, further work needs to be done using pP as a depth constraint with real data. Methods have to be worked out for making best use of the depth phase information in the signal arrival queue, and probably for making a choice of different algorithms. In some cases no uses at all would be made of pP and sP, and automatic methods to determine that this would be the best strategy needed.

We believe that the capabilities of AA ought to be expanded to include and make use of regional phases. There are six local phases: Pn, Pg, P, Sn, Sg and S. The program ACLOC uses regional phases as well as array information and other later phases for location. ACLOC would replace HYPO in AA. Conceptually, this is fairly straight-forward, but considerable programming effort is required to make the resulting large package manageable.

REFERENCES

Breding, D. R. (1982). Data User's Guide for the Regional Seismic Test Network (RSTN). Sandia National Laboratories, Albequerque, N. M., SAND-82-2935.

Bungum, H. (1983), L. B. Tronrud (ed) (1983). NORSAR Scientific Report No. 2-82/83 Semianual Technical Summary (June 1983).

Fix, J. E. (1972). Ambient Earth Motion in the Period Range from 0.1 to 2560 Sec BSSA 62 No 6 pp 1753-1760.

Herrin, E. (1982). The resolution of Seismic Instruments Used in Treaty Verification Research. BSSA 72 #6 pp S61-S67.

Openheim, A. V. and R. W. Schafer (1975). Digital Signal Processing, Prentice - Hall 585 pages

Owens, T. J., S. R. Taylor and G. Zandt (1983). Crustal Structure beneath RSTN stations Inferred from Teleseismic P-waveforms. Preliminary results at RSCP, RSSD, and RSNY, VCID-19859

Ringdal, F. (1976). Maximum likelihood estimation of seismice magnitude, Bull. Seism. Soc. Am. 66, 789-802.

Rodgers, P. W. and M. Hummel (1981). National Seismic Stations transducers and filters, Lawrence L. N. L., Livermore, Ca. VCRL-53093

Seismic Research Information System (SRIS), Program Specification for Automatic Association (1982). Geotech Alexandria Laboratory, Alexandria, Va.

Taylor, S. R. and B. J. Qualheim (1983). Regional Seismic Test Network Site Descriptions, Lawrence Livermore Laboratory Report - VCID-19769

(THIS PAGE INTENTIONALLY LEFT BLANK)

APPENDIX I

AMPLITUDES AND PERIODS AT RSTN STATIONS

ANK HSCP Delta = 5.44, Azimuth = 287.59, 83/018/0250:48.3														
	SP				BP					LP				
Phase	Amp	T(sec)	(S/N)	F(Hz)	Phase	Amp	T(sec)	(S/N)	F(Hz)	Phase	Amp	T(sec)	(S/N)	F(Hz)
Pz	42	0.325	29	4.0	Pz	20	2.5	187	1.63	-	-	-	-	-
Pn	14	0.25	15	3.4	Pn	9	3.5	100	1.62	-	-	-	-	-
Pe	24	0.325	20	2.5	Pe	17	3.0	20	1.63	-	-	-	-	-
Lgz	864	0.275	333	1.9	Lgz	91	0.75	145	1.57	-	-	-	-	-
Lgn	576	0.35	250	2.8	Lgn	95	1.0	95	1.71	-	-	-	-	-
Lge	581	0.225	364	4.3	Lge	36	0.5	285	1.57	-	-	-	-	-

ANK HSNT Delta = 30.71, Azimuth = 148.37, 83/018/0250:40.3														
	SP				BP					LP				
Phase	Amp	T(sec)	(S/N)	F(Hz)	Phase	Amp	T(sec)	(S/N)	F(Hz)	Phase	Amp	T(sec)	(S/N)	F(Hz)
Lgz	3.8	1.47	-	-	-	-	-	-	-	-	-	-	-	-
Lgn	2.0	1.575	-	-	-	-	-	-	-	-	-	-	-	-
Lge	2.5	1.375	-	-	-	-	-	-	-	-	-	-	-	-

ANK HSNY Delta = 16.46, Azimuth = 361.44, 83/018/0250:43.3														
	SP				BP					LP				
Phase	Amp	T(sec)	(S/N)	F(Hz)	Phase	Amp	T(sec)	(S/N)	F(Hz)	Phase	Amp	T(sec)	(S/N)	F(Hz)
Pz	2.2	0.2	3	2.25	-	-	-	-	-	-	-	-	-	-
Pz	2.2	0.2	3	3.65	-	-	-	-	-	-	-	-	-	-
Pn	2.9	0.325	4	3.0	-	-	-	-	-	-	-	-	-	-
Pe	1.75	0.225	-	-	-	-	-	-	-	-	-	-	-	-
Lgz	9.8	0.85	15	2.1	Lgz	16	1.25	4	1.32	-	-	-	-	-
Lgn	13	0.675	13	2.8	Lgn	11	1.5	5	1.37	-	-	-	-	-
Lge	11	0.775	5	2.0	Lge	22	2.0	5	1.26	-	-	-	-	-

ANK HSON Delta = 15.71, Azimuth = 175.51, 83/018/0250:43.3														
	SP				BP					LP				
Phase	Amp	T(sec)	(S/N)	F(Hz)	Phase	Amp	T(sec)	(S/N)	F(Hz)	Phase	Amp	T(sec)	(S/N)	F(Hz)
Pz	3.0	0.25	10	2.7	-	-	-	-	-	-	-	-	-	-
Pz	3.0	0.25	5	6.0	-	-	-	-	-	-	-	-	-	-
Pn	1.4	0.35	6	4.1	-	-	-	-	-	-	-	-	-	-
Pe	1.0	0.225	3	6.0	-	-	-	-	-	-	-	-	-	-
Lgz	7	0.625	6	1.65	Lgz	27	1.75	15	1.29	-	-	-	-	-
Lgn	5	0.925	30	1.15	Lgn	31	2.0	10	1.25	-	-	-	-	-
Lge	29	1.1	30	1.65	Lge	58	1.75	30	.87	-	-	-	-	-

ANK HSSD Delta = 12.74, Azimuth = 193.48, 83/018/0250:42.3														
	SP				BP					LP				
Phase	Amp	T(sec)	(S/N)	F(Hz)	Phase	Amp	T(sec)	(S/N)	F(Hz)	Phase	Amp	T(sec)	(S/N)	F(Hz)
Pz	8.4	0.4	4	15	-	-	-	-	-	-	-	-	-	-
Pz	8.4	0.4	5	3.6	-	-	-	-	-	-	-		-	-
Pn	4.4	0.35	-	-	-	-	-	-	-	-	-	-	-	-
Pe	3.6	0.4	-	-	-	-	-	-	-	-	-	-	-	-
Lgz	18	0.575	40	1.5	Lgz	31	1.75	31	1.2	-	-	-	-	-
Lgn	35	0.675	17	1.25	Lgn	20	1.5	50	1.13	-	-	-	-	-
Lge	32	0.675	83	1.7	Lgn	35	1.2	45	1.265	-	-	-	-	-

CAL RSCP Delta = 35.05, Azimuth = 281.924, 03/188/2342:37.9														
	SP				MP					LP				
Phase	Amp	T(sec)	(S/N)	F(Hz)	Phase	Amp	T(sec)	(S/N)	F(Hz)	Phase	Amp	T(sec)	(S/N)	F(Hz)
Pz	383.3	0.6	17	1.35	Pz	580.4	2.25	800	.05	Pz	8827.7	21	10	.045
Pn	44.9	0.625	30	1.7	Pn	48.4	1.75	86	.05	Pn	1860.4	22	36	.04
-	-	-	-	-	-	-	-	-	-	Pn	1860.4	22	30	.17
Pe	188.3	0.75	140	1.7	Pe	262.1	1.75	300	.05	Pe	4374.6	21	200	.041
-	-	-	-	-	-	-	-	-	-	Pe	4374.6	21	40	.16
Lgz	478.1	2.625	57	.3	Lgz	6724.4	7.0	8000	.035	-	-	-	-	-
-	-	-	-	-	Lgz	6724.4	7.0	1286	.155	-	-	-	-	-
Lgn	440.6	2.65	350	.3	Lgn	14492.1	6.25	10000	.055	-	-	-	-	-
Lge	280.2	2.675	150	.3	Lge	5704.9	6.5	5000	.035	-	-	-	-	-
-	-	-	-	-	Lrz	30218.1	9.75	6000	.11	Lrz	95691.9	19	8400	.16
-	-	-	-	-	Lrn	9181.7	8.75	3333	.1	Lrn	185965	21	6000	.091
-	-	-	-	-	Lre	26363.2	9.75	10000	.1	Lre	60129.9	19	4000	.15

CAL RSNY Delta = 35.4, Azimuth = 276.6, 03/188/2342:37.9														
	SP				MP					LP				
Phase	Amp	T(sec)	(S/N)	F(Hz)	Phase	Amp	T(sec)	(S/N)	F(Hz)	Phase	Amp	T(sec)	(S/N)	F(Hz)
Pz	33.7	1.05	20	1.2	Pz	370.1	3.85	143	.036	Pz	3436.9	19.0	167	.1
Pn	6.87	0.6	3.75	1.3	Pn	36.1	3.85	14	.07	Pn	563.2	19.0	60	.035
Pe	21.1	1.0	11	1.0	Pe	227.2	2.75	154	.036	Pe	2691.8	20.0	266	.036
-	-	-	-	-	-	-	-	-	-	Pe	2691.8	20.0	63	.12
Lgz	114.5	2.975	58	3	Lgz	4004.8	6.25	2333	.03	-	-	-	-	-
Lgn	234.2	3.2	67	3	Lgn	9226.1	7.75	3846	.05	-	-	-	-	-
Lge	87.0	3.425	20	3	Lge	3591.3	7.0	2000	.03	-	-	-	-	-
-	-	-	-	-	Lrz	279420	10.0	4615	1.1	Lrz	113920.015.0	7000	.1	
-	-	-	-	-	Lrn	13676	11.85	8857	.09	Lrn	165297	20.0	5000	.048
-	-	-	-	-	Lre	20353.8	8.85	7500	1.1	Lre	78056.5	15.0	6667	.033
-	-	-	-	-	-	-	-	-	-	Lre	78056.5	15.0	4714	.11

CAL RSCT Delta = 34.677, Azimuth = 268.75, 03/188/2342:37.9														
	SP				MP					LP				
Phase	Amp	T(sec)	(S/N)	F(Hz)	Phase	Amp	T(sec)	(S/N)	F(Hz)	Phase	Amp	T(sec)	(S/N)	F(Hz)
Pz	205.3	0.575	400	1.2	Pz	2114.9	3.75	667	.04	Pz	18385.5	21	1000	.03
-	-	-	-	-	Pz	2114.9	3.75	40	1.0	-	-	-	-	-
Pn	34.7	0.6	100	1.6	Pn	816.9	3.0	888	.04	Pn	4914.3	84	886	.04
-	-	-	-	-	Pn	816.9	3.0	14	.08	-	-	-	-	-
Pe	163.9	0.675	500	1.5	Pe	1375.4	3.85	1200	.04	Pe	10081.7	85	1000	.04
-	-	-	-	-	Pe	1375.4	3.85	85	1.0	-	-	-	-	-
Lgz	198.1	2.725	250	3	Lgz	5052.0	6.0	8667	.03	-	-	-	-	-
-	-	-	-	-	Lgz	5052.0	6.0	136	.89	-	-	-	-	-
Lgn	114.2	2.925	222	3	Lgn	6997.9	5.0	3333	.045	-	-	-	-	-
-	-	-	-	-	Lgn	6997.9	5.0	400	.81	-	-	-	-	-
Lge	130.9	3.2	222	.3	Lge	2529.2	4.75	8000	.095	-	-	-	-	-
-	-	-	-	-	Lge	25292.2	4.75	300	.85	-	-	-	-	-
-	-	-	-	-	Lrz	30210.1	10.6	8571	.1	Lrz	190188.0	13	4886	.038
-	-	-	-	-	Lrn	22760.9	10.0	8929	.1	Lrn	197068.9	16	4167	.035
-	-	-	-	-	Lre	21145.1	10.0	80000	.075	Lre	111307	15	4000	.04

CAL [illegible] Delta = 14.68, Azimuth = 243.18, [illegible]														
SP					SP					LP				
Phase	Amp	T(sec)	(S/N)	F(Hz)	Phase	Amp	T(sec)	(S/N)	F(Hz)	Phase	Amp	T(sec)	(S/N)	F(Hz)
Pz	84.4	1.275	62.5	.75	Pz	1485.2	4.25	500	.08	Pz	82667.7	18	7143	.056
Pz	-	-	-	-	Pz	1485.2	4.25	90	1.2	Pz	82667.7	18	889	.18
Pn	58.0	1.25	30	.75	Pn	842.6	3.75	850	.08	Pn	10601.6	18	909	.083
-	-	-	-	-	Pn	842.6	3.75	40	1.3	Pn	10601.6	18	850	.1
Pe	88.8	1.065	14	.78	Pe	1475.6	3.5	1333	0.7	Pe	82973.0	18	1333	.08
-	-	-	-	-	Pe	1475.6	3.5	185	.06	Pe	82973.0	18	8000	.01
Lgz	488.3	1.56	454	.3	Lgz	12573.8	5.25	8500	.03	-	-	-	-	-
-	-	-	-	-	Lgz	12573.8	5.25	454	.07	-	-	-	-	-
Lgn	485.0	1.475	800	.8	Lgn	8888.2	5.0	4000	.005	-	-	-	-	-
Lge	380.6	1.56	850	1.1	Lge	6885.12	5.0	8500	.045	-	-	-	-	-
-	-	-	-	-	Lrz	30818	8.75	8000	.1	Lrz	105857	83	5556	.043
-	-	-	-	-	-	-	-	-	-	Lrz	105857	83	8000	.16
-	-	-	-	-	Lrn	30818	10	10000	.1	Lrn	107388	19	6666	.031
-	-	-	-	-	-	-	-	-	-	Lrn	107388	19	10555	.019
-	-	-	-	-	Lre	30818	8.50	14888	.1	Lre	141083	17	13333	.028
-	-	-	-	-	-	-	-	-	-	Lre	141083	17	88571	.028

CASPX RSCI Delta = 19.80, Azimuth = 39.61, 83/017/1935:51.0														
	SP				MP					LP				
Phase	Amp	T(sec)	(S/N)	F(Hz)	Phase	Amp	T(sec)	(S/N)	F(Hz)	Phase	Amp	T(sec)	(S/N)	F(Hz)
Pz	14.6	0.325	-	-	Pz	-	-	-	-	-	-	-	-	-
Pn	6.7	0.325	-	-	Pn	-	-	-	-	-	-	-	-	-
Pe	11.4	0.325	-	-	Pe	-	-	-	-	-	-	-	-	-
Lgz	49.4	0.7	8	1.3	Lgz	41.9	1.5	6	1.2	-	-	-	-	-
Lgn	34.4	0.65	8	1.3	Lgn	35.0	1.5	6	1.1	-	-	-	-	-
Lge	33.5	0.625	6	1.3	Lge	26.0	1.75	6	1.275	-	-	-	-	-
-	-	-	-	-	-	-	-	-	-	Lrz	76.9	19.0	-	-
-	-	-	-	-	-	-	-	-	-	Lrn	59.9	23.0	2.5	.037
-	-	-	-	-	-	-	-	-	-	Lre	46.2	20.0	-	-

CASPX RSNT Delta = 89.16, Azimuth = 94.87, 83/017/1935:51.0														
	SP				MP					LP				
Phase	Amp	T(sec)	(S/N)	F(Hz)	Phase	Amp	T(sec)	(S/N)	F(Hz)	Phase	Amp	T(sec)	(S/N)	F(Hz)
Pz	1.3	0.5	?	?	-	-	-	-	-	-	-	-	-	-
Pn	-	-	2	2.3	-	-	-	-	-	-	-	-	-	-
Pe	1.1	0.65	4	2.7	-	-	-	-	-	-	-	-	-	-
Lgz	14.3	1.475	6	1	Lgz	17.3	1.5	20	1.07	-	-	-	-	-
Lgn	21.6	1.0	2	2	Lgn	34.6	1.5	50	1.12	-	-	-	-	-
Lge	11.4	1.15	16	1.7	Lge	8.0	1.5	31	1.1	-	-	-	-	-

CASPX RSNY Delta = 6.9, Azimuth = 45.84, 83/017/1935:51.0														
	SP				MP					LP				
Phase	Amp	T(sec)	(S/N)	F(Hz)	Phase	Amp	T(sec)	(S/N)	F(Hz)	Phase	Amp	T(sec)	(S/N)	F(Hz)
Pz	21.9	0.25	84	4.2	Pz	-	-	4.4	1.07	-	-	-	-	-
Pz	21.9	0.25	35	7.1	-	-	-	-	-	-	-	-	-	-
Pn	17.2	0.35	25	4.1	Pn	-	-	5	1.1	-	-	-	-	-
Pe	15.6	0.325	33	4.3	Pe	-	-	4.2	1.1	-	-	-	-	-
Pe	15.6	0.325	25	8.4	-	-	-	-	-	-	-	-	-	-
Lgz	207.8	0.475	60	2.1	Lgz	146.1	1.5	26.7	1.17	-	-	-	-	-
Lgn	175.0	0.55	60	1.65	Lgn	164.0	1.0	36	1.27	-	-	-	-	-
Lgn	175.0	0.55	50	6.3	-	-	-	-	-	-	-	-	-	-
Lge	212.0	0.75	75	1.6	Lge	283	1.0	70	1.18	-	-	-	-	-
Lge	212.0	0.75	50	5.8	-	-	-	-	-	-	-	-	-	
-	-	-	-	-	-	-	-	-	-	Lrz	141.5	11.0	4.3	.051
-	-	-	-	-	-	-	-	-	-	Lrn	1110	12.0	2.2	.047
-	-	-	-	-	-	-	-	-	-	Lre	110.0	9.0	5.0	.04

CASPX RSON Delta = 17.91, Azimuth = 65.41, 83/017/1935:51.0														
	SP				MP					LP				
Phase	Amp	T(sec)	(S/N)	F(Hz)	Phase	Amp	T(sec)	(S/N)	F(Hz)	Phase	Amp	T(sec)	(S/N)	F(Hz)
Pz	2.3	0.85	6.7	4.4	Pz	-	-	-	-	-	-	-	-	-
Pn	1.3	0.3	10	4.3	Pn	-	-	-	-	-	-	-	-	-
Pe	0.9	0.35	10	4.3	Pe	-	-	-	-	-	-	-	-	-
Lgz	62.2	0.625	67	1.6	Lgz	36.6	1.25	22	1.17	-	-	-	-	-
-	-	-	-	-	Lgz	36.6	1.25	40	1.45	-	-	-	-	-
Lgn	46.6	0.7	100	1.5	Lgn	53.4	1.0	40	1.15	-	-	-	-	-
Lge	46.9	0.725	62	1.55	Lge	33.1	1.5	16	1.06	-	-	-	-	-
-	-	-	-	-	Lge	33.1	1.5	40	1.49	-	-	-	-	-
-	-	-	-	-	-	-	-	-	-	Lrz	57.6	16.0	2.66	.056
-	-	-	-	-	-	-	-	-	-	Lrn	73.5	15.0	-	-
-	-	-	-	-	-	-	-	-	-	Lre	41.6	15.0	2.5	.056

[illegible] Delta = 81.8, Azimuth = [illegible]														
SP					MP					LP				
Phase	Amp	T(sec)	(S/N)	F(Hz)	Phase	Amp	T(sec)	(S/N)	F(Hz)	Phase	Amp	T(sec)	(S/N)	F(Hz)
Pz	747.9	0.625	666.6	1.6	Pz	672.3	1.75	200	.07	Pz	31791.6	17.0	625	.043
-	-	-	-	-	Pz	672.3	1.75	100	.98	-	-	-	-	-
Pn	365.5	0.55	666.6	2.0	Pn	354.2	1.5	375	.09	Pn	19059.6	20.0	600	.036
-	-	-	-	-	Pn	354.2	1.5	66.6	.79	-	-	-	-	-
Pe	661.7	0.6	500.0	2.0	Pe	159.6	1.25	100	.065	Pe	10350.6	16.0	1633	.04
Lgz	-	-	114	1.6	-	-	-	-	-	-	-	-	-	-
Lgn	-	-	200	1.7	-	-	-	-	-	-	-	-	-	-
Lge	-	-	233.3	1.9	-	-	-	-	-	-	-	-	-	-
-	-	-	-	-	Lrz	4699.3	32.5	10000	.035	Lrz	165927	33	10000	.035
-	-	-	-	-	Lrn	8961.1	30.5	3333	.035	Lrn	131016.089.0	6666	.035	
-	-	-	-	-	Lre	5692.3	34.5	50003	.035	Lre	165327	36.0	10000	.035

MEX RENT Delta = 46.84, Azimuth = 164.72, 83/084/0017:38.6														
SP					MP					LP				
Phase	Amp	T(sec)	(S/N)	F(Hz)	Phase	Amp	T(sec)	(S/N)	F(Hz)	Phase	Amp	T(sec)	(S/N)	F(Hz)
Pz	91.9	0.675	333.3	2.0	Pz	1524.2	3.0	100	.04	Pz	3052.1	14.0	220	.032
-	-	-	-	-	Pz	1524.2	3.0	250	1.0	-	-	-	-	-
Pn	46.9	0.55	400	1.4	Pn	807.5	3.0	100	.06	Pn	1763.5	13.0	26.6	.041
-	-	-	-	-	Pn	807.5	3.0	151.5	1.0	-	-	-	-	-
Pe	30.5	0.65	400	1.2	Pe	368.0	3.0	5.5	.055	Pe	660.5	14.0	40	.046
-	-	-	-	-	Pe	389.0	3.0	131.5	.92	-	-	-	-	-
Lgz	29.9	2.675	10	.6	Lgz	1767.3	7.25	-	-	-	-	-	-	-
Lgn	33.6	2.575	15	1.0	Lgn	1311.4	7.25	-	-	-	-	-	-	-
Lge	53.2	2.675	10	.3	Lge	2362.1	6.5	-	-	-	-	-	-	-
-	-	-	-	-	Lrz	3615.6	9.0	6000	.05	Lrz	76476.5	31	6000	.035
-	-	-	-	-	Lrn	2316.9	10.75	333	.04	Lrn	53901.2	26	450	.05
-	-	-	-	-	Lre	5671.6	11.75	1363.6	.03	Lre	105666	34	3750	.046

MEX HENY Delta = 33.27, Azimuth = 216.85, 83/084/0017:38.6														
SP					MP					LP				
Phase	Amp	T(sec)	(S/N)	F(Hz)	Phase	Amp	T(sec)	(S/N)	F(Hz)	Phase	Amp	T(sec)	(S/N)	F(Hz)
Pz	137.9	0.925	60	1.15	Pz	332.9	1.5	40	.06	Pz	1642.6	17	100	.044
-	-	-	-	-	Pz	332.9	1.5	55	.99	-	-	-	-	-
Pn	67.9	0.925	30	1.3	Pn	165.1	1.25	31	.1	Pn	1210.3	20	300	.035
Pn	67.9	0.925	27.2	2.6	Pn	165.1	1.25	50	.955	-	-	-	-	-
Pe	38.6	1.0	25	2.5	Pe	1291.1	1.3	14.3	.05	Pe	630	17	150	.033
-	-	-	-	-	Pe	1291.1	1.3	40	.96	-	-	-	-	-
-	-	-	-	-	Lrz	4827	26	1111.1	.04	Lrz	151697	27	5555.5	0.39
-	-	-	-	-	Lrn	3472.3	24.25	1111.1	.04	Lrn	106931	24	20000	0.36
-	-	-	-	-	Lre	3312.7	31.5	3433.3	.035	Lre	136292	29	25000	0.35

[redacted] Delta = 34.6, Azimuth = [redacted], 83/084/0817:38.6													
SP					MP					LP			
Phase	Amp	T(sec)	(S/N)	F(Hz)	Phase	Amp	T(sec)	(S/N)	F(Hz)	Phase	Amp	T(sec)	(S/N)	F(Hz)
Pz	504.4	0.95	500	1.5	Pz	1325.3	2.0	75	.04	Pz	4108.6	22.0	200	.041
-	-	-	-	-	Pz	1325.3	2.0	333.3	.97	-	-			
Pn	166.1	1.025	300	1.9	Pn	625.1	2.3	100	.035	Pn	2598.6	23.0	125	.041
-	-	-	-	-	Pn	625.1	2.3	142.8	.97	-	-	-	-	
Pe	22.6	0.57	400	1.9	Pe	54.6	1.5	10	.04	Pe	252.9	17.0	150	.041
-	-	-	-	-	Pe	54.6	1.5	100	.86	-	-	-	-	
Lgz	72.7	3.85	54.5	.4	-	-	-	-	-	-	-	-	-	
Lgz	72.7	3.85	20	.6	-	-	-	-	-	-	-	-	-	
Lgn	83.4	2.80	28.6	.35	-	-	-	-	-	-	-	-	-	
Lge	67.3	3.025	40	.35	-	-	-	-	-	-	-	-	-	-
Lge	67.3	3.025	30	1.2	-	-	-	-	-	-	-	-	-	-
-	-	-	-	-	Lrz	4416.4	6.25	1400	.035	Lrz	55187.5	27.0	6000	.04
-	-	-	-	-	-	-	-	-	-	Lrz	55187.5	27.0	114.3	.091
-	-	-	-	-	Lrn	3110.3	6.5	2000	.035	Lrn	49576.6	31.0	4600	.039
-	-	-	-	-	-	-	-	-	-	Lrn	49576.6	31.0	100	1
-	-	-	-	-	Lre	4265.4	7.0	2000	.03	Lre	71656.5	40.0	14285.7	.025
-	-	-	-	-	-	-	-	-	-	Lre	71656.5	40.0	1570	.09

[redacted] Delta = 35.06, Azimuth = 162.86, 83/084/0817:39.6													
SP					MP					LP			
Phase	Amp	T(sec)	(S/N)	F(Hz)	Phase	Amp	T(sec)	(S/N)	F(Hz)	Phase	Amp	T(sec)	(S/N)	F(Hz)
Pz	108.7	1.525	50	1.3	Pz	549.7	3.85	350	.03	Pz	7921.3	25	666.6	.039
-	-	-	-	-	Pz	549.7	3.85	350	.03	Pz	7921.3	25	25	.03
Pn	189.7	1.575	666	1.3	Pn	553.1	2.85	700	.04	Pn	5990.4	25	333.3	.043
-	-	-	-	-	Pn	553.1	2.85	714	.85	Pn	5990.4	25	16.3	.03
Pe	74.7	1.2	66.6	1.1	Pe	130.6	1.75	100	.03	Pe	2073.4	25	200	.03
-	-	-	-	-	Pe	130.6	1.75	428.6	.86	Pe	2073.4	25	12.5	.09
Lgz	96.0	2.75	33.3	1.4	Lgz	1301.6	5.5	5000	.035	-	-	-	-	-
Lgn	114.4	1.75	66.6	1.2	Lgn	1557.6	5.75	5000	.03	-	-	-	-	-
Lge	179.3	2.975	50	1.1	Lge	6114.4	7.25	7000	.025	-	-	-	-	-
-	-	-	-	-	Lrz	3449.6	12.75	6000	.05	Lrz	70761.3	32	10000	.035
-	-	-	-	-	-	-	-	-	-	Lrz	70761.3	32	333	.09
-	-	-	-	-	Lrn	4036.16	6.75	7500	.06	Lrn	35427.7	29	10000	.045
-	-	-	-	-	-	-	-	-	-	Lrn	35427.7	29	200	.035
-	-	-	-	-	Lre	6114.4	7.25	8000	.04	Lre	136789.070	55333	625	
-	-	-	-	-	-	-	-	-	-	Lre	136789.070	500	09	

NTS HHCP Delta = 84.91, Azimuth = 282.47, 02/217/1402:03.0														
	SP				MP					LP				
Phase	Amp	T(sec)	(S/N)	F(Hz)	Phase	Amp	T(sec)	(S/N)	F(Hz)	Phase	Amp	T(sec)	(S/N)	F(Hz)
Pz	264	0.05	148.6	1.1	Pz	148	1.85	100	1.31	-	-	-	-	-
Pn	89	0.05	16.6	0.6	Pn	19	1.85	13.75	.76	-	-	-	-	-
-	-	-	-	-	Pn	19	1.85	16.0	1.3	-	-	-	-	-
Pe	86	0.05	80.0	10	Pe	86	1.1	37.5	.85	-	-	-	-	-
-	-	-	-	-	Pe	86	1.1	50.0	1.87	-	-	-	-	-
Lgz	98	8.45	22.5	.4	Lgz	167	8.5	11	.4	-	-	-	-	-
-	-	-	-	-	Lgz	167	8.5	10	.65	-	-	-	-	-
Lgn	880	8.05	90	.4	Lgn	706	8.75	50	.37	-	-	-	-	-
-	-	-	-	-	Lgn	706	8.75	62	.6	-	-	-	-	-
Lge	101	1.75	40	.4	Lge	168	3.0	30	.39	-	-	-	-	-
-	-	-	-	-	Lge	168	3.0	22.5	.6	-	-	-	-	-
-	-	-	-	-	Lrz	837	6.85	33	.16	-	-	-	-	-
-	-	-	-	-	Lrn	282	4.25	30	.36	-	-	-	-	-
-	-	-	-	-	Lre	184	5.0	50	.16	-	-	-	-	-

NTS HHNT Delta = 85.44, Azimuth = 162.64, 02/217/1402:03.0														
	SP				MP					LP				
Phase	Amp	T(sec)	(S/N)	F(Hz)	Phase	Amp	T(sec)	(S/N)	F(Hz)	Phase	Amp	T(sec)	(S/N)	F(Hz)
Pz	108	1.085	100	0.6	Pz	253	2.0	110	1.3	Pz	26	20	2.9	.115
Pn	97	1.05	66.6	1.6	Pn	192	1.75	85.7	.77	Pn	-	-	6.4	0.75
Pe	14	0.6	57	1.7	Pe	11	1.25	50	.95	Pe	-	-	2.7	.062
Lgz	36	8065	85	.4	Lgz	346	3.75	20	.83	-	-	-	-	-
Lgz	38	8065	12.5	6.0	Lgz	346	3.75	20	.46	-	-	-	-	-
Lgn	81	8.6	10.1	.35	Lgn	176	3.5	16.1	.22	-	-	-	-	-
Lgn	81	8.6	11.1	7.6	-	-	-	-	-	-	-	-	-	-
Lge	86	8.075	80.	.4	Lge	251	3.25	33.3	.12	-	-	-	-	-
Lge	66	8.075	40.	6.0	Lge	251	3.25	35.0	.46	-	-	-	-	-
-	-	-	-	-	Lrz	864	6.0	41.6	.065	Lrz	1360	16	54	.05
-	-	-	-	-	Lrn	199	6.0	27.8	.13	Lrn	953	17	60	.065
-	-	-	-	-	Lre	250	6.5	36.3	.19	Lre	384	17	36	.115

NTS HHNY Delta = 31.08, Azimuth = 271.12, 02/217/1402:03.0														
	SP				MP					LP				
Phase	Amp	T(sec)	(S/N)	F(Hz)	Phase	Amp	T(sec)	(S/N)	F(Hz)	Phase	Amp	T(sec)	(S/N)	F(Hz)
Pz	85	1.075	10	1.0	Pz	65	2.75	16	1.13	Pz	33	10	-	-
Pn	3.6	0.825	-	-	Pn	34	2.75	9	1.15	Pn	16	15	-	-
Pe	17	1.1	7	1.1	Pe	41	2.5	10	1.81	Pe	20	13	-	-
Lgz	37	1.075	15	.4	Lgz	146	2.75	10	.65	-	-	-	-	
Lgn	85	8.075	30	.4	Lgn	257	3.0	80	.66	Lg	-	-	-	-
Lge	25	1.75	7.1	.5	Lge	106	2.5	8.6	.46	-	-	-	-	
Lge	-	-	-	-	Lge	106	2.5	13.3	.66	-	-	-	-	-
Lrz	-	-	-	-	Lrz	765	10.85	62.5	.13	Lrz	2762	13	100	.09
Lrz	-	-	-	-	-	-	-	-	-	Lrz	2762	13	50	.115
Lrn	-	-	-	-	Lrn	136	7.0	16.8	.13	Lrn	485	13	84	.073
Lre	-	-	-	-	Lre	495	10.75	80	.14	Lre	2100	14	80	.08
Lre	-	-	-	-	-	-	-	-	-	Lre	2100	14	66.6	.151

NTS HSCN Delta = 81.04, Azimuth = 337.71, 08/217/1402:02.0														
SP					MP					LP				
Phase	Amp	T(sec)	(S/N)	F(Hz)	Phase	Amp	T(sec)	(S/N)	F(Hz)	Phase	Amp	T(sec)	(S/N)	F(Hz)
Pz	734	0.975	666.6	1.3	Pz	629	1.5	600	1.3	Pz	44	11.0	5	.05
-	-	-	-	-	-	-	-	-	-	Pz	44	11.0	3.3	.182
Pn	845	0.95	466.6	1.3	Pn	604	1.5	350	1.3	Pn	22	9.0	5	.165
Pe	836	1.0	500	1.3	Pe	290	1.5	1666	1.21	Pe	16	11.0	5	.207
Lgz	495	2.05	30	.5	Lgz	226	2.75	33.3	.69	-	-	-	-	-
Lgz	495	2.05	33	10.5	-	-	-	-	-	-	-	-	-	-
Lgn	15	1.4	16.3	.66	Lgn	156	2.75	12.2	.66	-	-	-	-	-
Lgn	15	1.4	15.0	10.3	-	-	-	-	-	-	-	-	-	-
Lge	75	1.6	41.6	.7	Lge	264	2.25	44.4	.61	-	-	-	-	-
Lge	75	1.6	15.0	10.6	-	-	-	-	-	-	-	-	-	-
-	-	-	-	-	Lrz	477	7.25	75	.06	Lrz	871	13	50	.05
-	-	-	-	-	-	-	-	-	-	Lrz	871	13	54.5	.13
-	-	-	-	-	Lrn	340	6.75	60	.13	Lrn	622	13	57.1	.119
-	-	-	-	-	Lre	217	6.75	55.5	.18	Lre	413	13	35.7	.11

NTS HSSD Delta = 11.48, Azimuth = 336.37, 08/217/1400:03.0														
SP					MP					LP				
Phase	Amp	T(sec)	(S/N)	F(Hz)	Phase	Amp	T(sec)	(S/N)	F(Hz)	Phase	Amp	T(sec)	(S/N)	F(Hz)
Pez	293.1	0.675	450	1.1	Pz	229.1	1.75	466	.96	Pz	22.7	13.0	5.0	.255
Pez	-	-	-	-	-	-	-	-	-	Pz	E	13.0	5.0	.335
Pen	220.5	0.7	250	1.1	Pn	237.9	1.75	350	1.12	Pn	3.0	6.0	4.0	.255
Pen	-	-	-	-	-	-	-	-	-	Pn	3.0	6.0	10.0	.34
Pee	255.6	0.925	525	1.1	Pe	284.6	1.75	350	.9	Pe	12.3	11.0	6.3	.255
Pee	-	-	-	-	-	-	-	-	-	Pe	12.3	11.0	6.6	.34
Lgz	339	1.5	500	.7	Lgz	573	2.25	5671	.64	-	-	-	-	-
Lgn	352	1.425	265	.7	Lgn	666	2.25	200	.55	-	-	-	-	-
Lge	266	1.45	250	1.3	Lge	656	1.75	200	.66	-	-	-	-	-
-	-	-	-	-	Lrz	615	6.5	100	.14	Lrz	3565	15	16	.015
-	-	-	-	-	Lrn	696	4.5	60	.17	Lrn	1555	15	6.6	.085
-	-	-	-	-	Lrn	696	4.5	100	.56	-	-	-	-	-
-	-	-	-	-	Lre	716	6.75	125	.1	Lre	2407	14	12.5	.085
-	-	-	-	-	Lre	716	6.75	166.6	.5	-	-	-	-	-

[redacted] Delta = [redacted], Azimuth = [redacted]														
	SP					MP					LP			
Phase	Amp	T(sec)	(S/N)	F(Hz)	Phase	Amp	T(sec)	(S/N)	F(Hz)	Phase	Amp	T(sec)	(S/N)	F(Hz)
Pz	-	-	-	-	Pz	-	-	-	-	Pz	-	-	-	-
Pn	-	-	-	-	Pn	Cal	-	-	-	Pn	Cal	-	-	-
Pe	-	-	-	-	Pe	-	-	-	-	Pe	-	-	-	-
Lez	4.6	2.185	-	-	Lez	-	-	-	-	-	-	-	-	-
Lzn	7.1	1.675	60	2.0	Lzn	-	-	-	-	-	-	-	-	-
Lze	4.95	2.2	-	-	Lze	-	-	-	-	-	-	-	-	-

[redacted] Delta = [redacted], Azimuth = [redacted]														
	SP					MP					LP			
Phase	Amp	T(sec)	(S/N)	F(Hz)	Phase	Amp	T(sec)	(S/N)	F(Hz)	Phase	Amp	T(sec)	(S/N)	F(Hz)
Pz	10.4	0.8	10.5	5.7	Pz	-	-	5.4	.88	Pz	-	-	-	-
Pz	10.4	0.8	11.6	7.4	-	-	-	-	-	-	-	-	-	-
Pn	7.3	0.175	10	4.6	Pn	Cal	-	-	-	Pn	Cal	-	-	-
Pn	7.3	0.175	15.6	6.5	-	-	-	-	-	-	-	-	-	
Pe	3.1	0.15	9.1	4.7	Pe	-	-	-	-	Pe	-	-	-	-
Lez	64.6	0.2	50	4.6	Lez	-	-	5.0	1.4	-	-	-	-	-
Lzn	54.5	0.2	100	5.0	Lzn	-	-	-	-	-	-	-	-	-
Lze	76.9	0.225	100	5.0	Lze	-	-	13.3	1.04	-	-	-	-	-

APPENDIX II

DYNAMIC-KINEMATIC CRITERIA FOR EVENT REALITY

A BETTER APPROACH TO HANDLING AMPLITUDE DATA AA

M E M O R A N D U M

TO: A. Kerr, W. Dean, J. Gonez, R. North, R. Slunga, R. Shumway

FROM: R. Blandford

SUBJECT: Dynamic-Kinematic Criteria for Event Reality

DATE: 7 October 1982

We now have a complete "system" for dynamic-kinematic amplitude checking; attached to this memo. I think this system could be checked out fairly well with the artificial data John Gonez and I are generating. The subroutine amp may diverge if very large or small ID = 1 type values are in the data. Bob Shumway and I will soon distribute an improved version of amp. I think this code is in a "final" state suitable for use in existing AA programs. Only the I/O needs to be modified, and this is fairly well isolated in the event.f and mkpkin.f files.

As long as we are talking about AA, I propose a measure of AA quality, "Association Percentage" defined as follows. Define events which are to be detected; e.g. events with 5 non-array stations; plus events with two arrays and one confirming station, plus events with 2 P waves and one S, etc. All arrivals in this set of events when perfectly analyzed constitute the "base set of arrivals". Now we go down the perfect bulletin and pick out the first event. Is there an event in the AA with (75%) of the arrivals. (Obviously 75% is a variable; probably anywhere between 60% and 90% is alright.) If so, then all correct arrivals in that AA event may be added to the total correct arrivals count; and all incorrectly associated arrivals should be subtracted. I propose that a correctly associated arrival should count even if the phase name is incorrect. (Or perhaps it should get 1/2 or 0 weight if incorrectly identified.) In this way all "perfect bulletin" events are considered. Any remaining arrivals which have been associated into events (which are, presumably "false" or "bad" events and which will give an analyst severe trouble to clean up) will be subtracted from the total correct arrivals count. The Association Percentage is calculated as (total correct arrivals count)/(base set of arrivals).

This measure:

Doubly penalizes the creation of false events and incorrect association to good events.
Rewards correct identification of later phases.
Does not depend on location error which is highly variable depending on event size and travel-time residuals.
Can be easily calculated automatically.
Perhaps too severely penalizes splitting large events, especially an equal split.

INTRODUCTION

The problem of verifying that magnitude estimators for events which have been created by an automatic association (AA) routine are based on a reasonable subset of detecting and non-detecting stations has been considered by Elvers (1980). She developed a "plausibility function" for the amplitude distributions which is essentially proportional to the likelihood of observing a particular configuration of amplitudes when the event is assumed to have occurred.

In this discussion, we attempt to improve several aspects of this procedure. As a computational improvement we also have developed a Newton-Raphson procedure for computing the maximum likelihood magnitude, assuming the signal and noise variances are known. This procedure runs much faster than the search techniques used by previous authors.

We also give a method for discarding single stations with outlying amplitudes (I, see Figure 1) based on the "influence" they exert on the magnitude estimator. This replaces the Elvers procedure of comparing the separate components of the likelihood for the purpose of determining the influential stations. Our procedure for discarding stations is also apparently not so likely to "destroy" the event in the case that a large number of stations are "down" and fail to report, but do not inform the bulletin analysis center of this fact.

Slunga (personal communication, 1982) has pointed out that the "dynamic" amplitude criteria of Elvers seem to erroneously discard arrivals from an event on the basis of amplitude anomalies. On occasion, although the amplitudes are indeed anomalous, the probability that the arrival time could agree by accident seems even smaller, so that it seems unreasonable to totally discard the arrival from the event.

To help remedy this paradox we propose to measure the overall event plausibility with a "kinematic" likelihood ratio (II) in parallel with the dynamic one. If the dynamic criteria suggest that an observed amplitude is unreliable but the kinematic criteria are favorable, then we suggest that the appropriate procedure in most cases is to assume

that there is some error in the amplitude measurement and to recalculate the magnitude, after making an appropriate change in the amplitude data, but to continue to use the reported arrival time for estimation of location.

Finally, we have developed a procedure for tying these new computational techniques together. In general terms this procedure is not derived from theoretical considerations but embodies common sense ideas about the causes of erroneous amplitude measurements.

It is important to emphasize that these techniques cannot simply be inserted into an automatic association program as mathematical routines like, for example, the cosine function. Instead the routines contain parameters which are specific to the network, detectors, and methods of analysis. These parameters must be determined by careful statistical analysis of network bulletins which are relatively error-free, and by analysis of false events produced by the automatic association program in which they are to be used.

FUNCTIONAL DESCRIPTION

In Figure 1 we see a flow chart of the proposed procedure. The Roman numerals I-II denote the computational techniques referred to in the Introduction.

At the top of Figure 1 we see that the event is submitted to the program for analysis. Obviously only those events should be accepted for which the program is prepared. For example we may anticipate that the first version of the program will be prepared to work only on initial P waves. If the event is made up of Pg, S, Lg, etc. then the algorithm has nothing to contribute. On the other hand an event with only one P wave and without an amplitude reading may be submitted. The single detection might be unlikely because many stations with lower thresholds nearby the detecting station did not detect. When this P wave is discarded then the event might be unreliable on kinematic grounds.

The event data is then submitted to a subroutine (I) which computes the Ringdal magnitude and detects outlying magnitudes. In Appendix I is a discussion and listing of a subroutine (amp) which rapidly computes the Ringdal magnitude given station amplitudes and thresholds in terms of magnitudes, and assuming that the signal and noise variances are known. Before this subroutine can be used, of course, distance-amplitude relations must be used to transform amplitudes and thresholds to magnitudes.

The amplitude patterns can be subdivided roughly into n_1 observed amplitudes, n_2 above the noise threshold and with arrival times but not amplitudes reported, and n_3 below the noise threshold and not detected. Of course other subcategories such as clipping might be added. For the general unknown magnitude case the log-likelihood as given by Elvers (1980) would be of the form:

$$\ln L(m) \doteq -\frac{n_1}{2}\ln\sigma_s^2 - \frac{1}{2\sigma_s^2}\sum_{j=1}^{n_1}(m_j - m)^2 + \sum_{j=1}^{n_2}\ln\Phi(\tilde{t}_j) + \sum_{j=1}^{n_3}\ln\Phi(-\tilde{t}_j) \qquad (1)$$

FLOW CHART FOR DYNAMIC-KINEMATIC ANALYSIS FOR AUTOMATIC ASSOCIATION

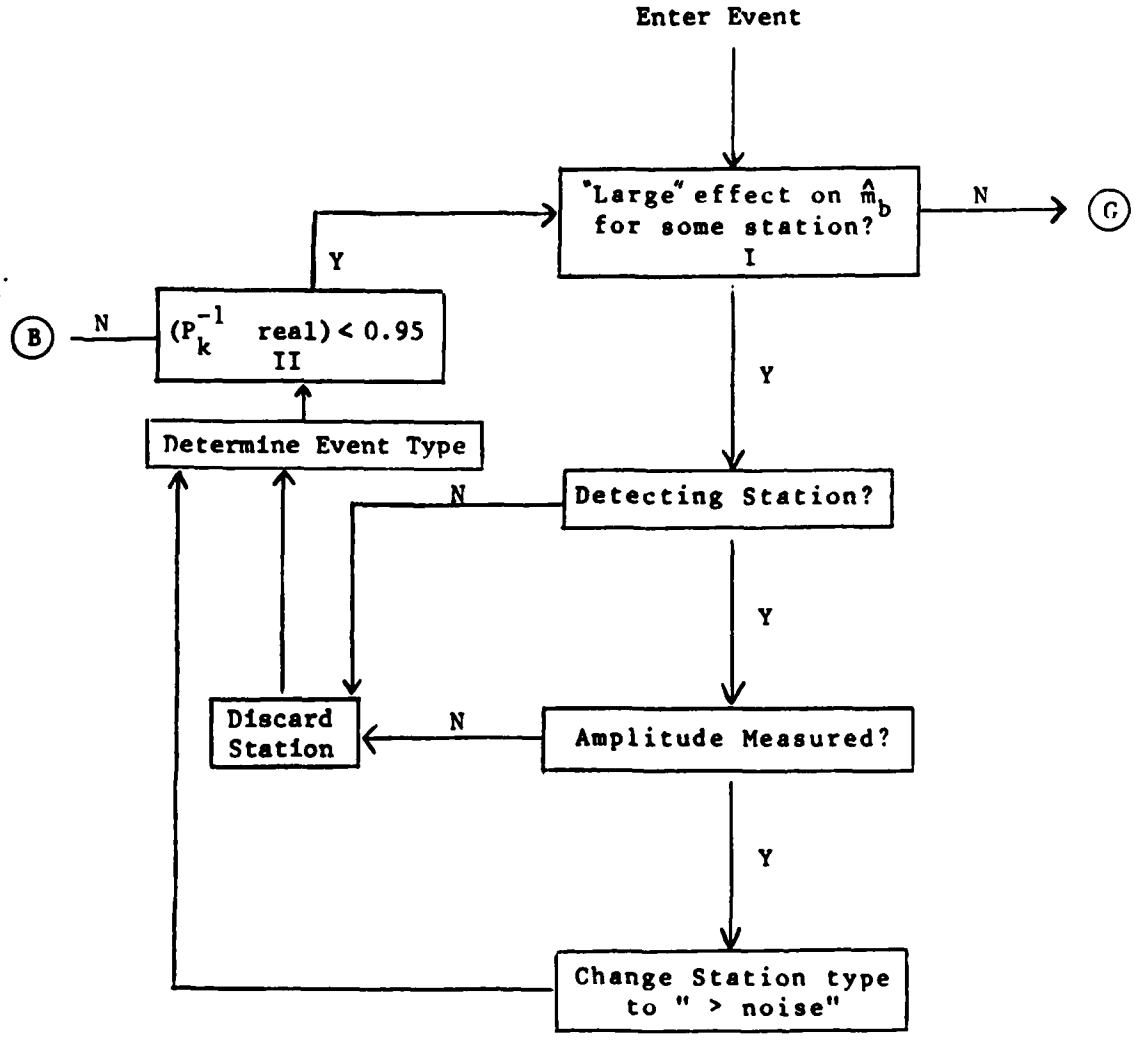

Pa - Amplitude probability	(G) - Good event exit
Pk^{-1} - Kinematic probability with one less station if a suspect station has been removed	(B) - Bad event exit

Figure 1.

where m_j are the observed amplitudes, m is the theoretical magnitude and:

$$z_j = \frac{m - \bar{D}_j - C}{\sqrt{\sigma_s^2 + \sigma_j^2}}$$

is a standard value depending on the mean noise level $\bar{D}_j$ with variance σ_j^2, the theoretical magnitude m with observed variance σ_s^2, and a signal-to-noise constant C. Since m is the only unknown, (1) can be maximized using the Newton-Raphson or scoring algorithms, which leads to the maximum likelihood estimator m and its estimated variance $\hat{\sigma}_{\hat{m}}^2$ (see Appendix I). The above approach is essentially that followed by Elvers (1980).

As a modification to the above Elvers (1980) suggests comparing the value of the maximized log likelihood, say ln $L(\hat{m})$ with some arbitrary threshold, with the first component of (1) modified to behave like an estimated interval probability. If the total plausibility, say ln $L(\hat{m})$ is too small, then the event can be rejected. The other decision that can be made at this point in the Elvers procedure is to discard a single station value based on a single station component of ln $L(\hat{m})$. For example the decision to reject a station j which does not observe is based on the value of $\ln(\Phi(-z_j))$, which is the probability of observing a value below the noise threshold at the jth station.

The problem, mentioned by Elvers (1980), with this approach is that the total plausibility depends in part upon point values of the density and in part upon interval probabilities which are integrated densities. Thus it is likely that eliminating an event purely on this criterion will unnecessarily eliminate events. The problem is magnified when one uses the Elvers (1980) procedure to eliminate single stations; purely on the basis of their plausibility values.

As a better method for detecting station outliers, we suggest recalculating the magnitude estimator with each station value missing to obtain, say $m_{(-i)}$ for i=1,...,n, where $m_{(-i)}$ denotes the magnitude estimated when station i is left out of the calculation. These can be compared with the original estimator, say m, to determine the "influence

of station i. For example, a common measure of influence is "Cook's distance", defined in this case by:

$$z_{(-i)} = \frac{\hat{m} - \hat{m}_{(-i)}}{\hat{\sigma}_{\hat{m}}} \qquad (2)$$

An heuristic procedure suggested by Cook is to reject station i when $z_{(-i)}$ moves further away from zero than $z(\alpha/2)$, where α is some arbitrary probability value.

As an example of how the two procedures for amplitude verification might work in practice, consider the 11 station "event", shown schematically in Table 1. We note first that taking the simple mean of the observed magnitudes yields $\overline{m} = 4.04$, whereas the maximum likelihood estimator is $\hat{m} = 3.78$ with estimated standard deviation $\hat{\sigma}_{\hat{m}} = .12$ so that the censored observations definitely pull the estimator down.

In order to determine whether any of the station values m_i are outliers, we may use the analogue of Cook's distance given in equation (2). The estimated deleted station magnitudes $\hat{m}_{(-i)}$ for i=1,2,...,11 are shown in Table 1 and we note that the greatest change is produced by omitting station 6($\hat{m}_{-6} = 3.89$) which is the value known to be below its noise threshold $\overline{D}_3 = 3$. The elimination of this station then moves the maximum likelihood estimator back towards the mean.

A program, DETZ, which produces the values of $z_{(-i)}$ is given in Appendix I.

TREATMENT OF STATIONS WITH ANOMALOUS AMPLITUDES

Returning to Figure 1 we must ask what course of action to take when an anomalous station amplitude is discovered by procedure I. First we determine if the most anomalous station has reported a detection or if, as in Table 1, it has simply failed to report at all, implying that the signal level is below the noise level. In the latter case we follow the approach suggested by Elvers (1980) and simply discard the station. However, we may look ahead a bit and note that, unlike Elvers we

TABLE 1

MAXIMUM LIKELIHOOD ESTIMATORS FOR MAGNITUDE

Case I	i	Data	$\hat{m}_{-i}$	$\hat{\sigma}_{\hat{m}}$	lnL	$z_{(-i)}$
Station	1	4.0	3.74	.13	1.03	.32
	2	3.6	3.80	.12	.96	-.25
	3	4.4	3.67	.13	2.27	.89
	4	4.0	3.74	.13	1.03	.32
	5	4.2	3.70	.13	1.51	.60
*	6	3.0	3.89	.17	6.14	-1.00
	7	4.0	3.80	.12	3.06	-.23
	8	4.2	3.79	.12	2.87	-.14
	9	3.9	3.81	.12	3.20	-.29
	10	4.5	3.78	.12	2.73	-.05
	11	5.0	3.78	.12	2.68	-.00
	Overall		3.78	.12	2.68	

immediately test for the kinematic probability of this event (II) and if the probability of the event being real is less than say 0.95 then we exit the routine with a bad event flag. That is, non-detection by this station suggests that there is something wrong with the event, and unless the kinematic probability is high the event is discarded. On the other hand, if the kinematic probability of the event is high, then probably there was something wrong at the station, and we return to further analyze the event without considering this station. Since in practice many stations fail to report due to operational consideration we should probably set a less restictive threshold for the non-detecting stations, that is, we should tend to reject them first. For example, if for a non-detecting station $z_{(-i)} \leq -0.7$ reject it (see Table I) but otherwise require $z_{(-i)} \geq 1.0$ for rejection. Probably we should have no anomalous non-detecting station remaining before considering other stations. Further work, perhaps empirical is needed to best determine those thresholds.

If the anomalous station did detect we ask if an amplitude was measured or not. If no amplitude was measured then we must have the situation where this station could not have been expected to detect; typically a station in a shadow zone to a small event. Again we discard the station and check the kinematic probability. Since we have by this time eliminated many of the incorrectly non-reporting stations, the event magnitude should not be biased too low so that stations should not be incorrectly thrown out at this point.

Finally we have the case where there <u>is</u> an amplitude measurement at the anomalous station: either it is too large or too small. In either case we assume that some blunder has been made and that if a true signal has been detected then the amplitude has been recorded or transmitted incorrectly. Thus we simply change the amplitude measurement (not in the original files of course) to state that the signal was greater than the noise. Again we proceed through the kinematic criterion. Note that if this event comes around again then this detection will not have a measured amplitude so that if it is unlikely that this station could have detected the event at all the arrival will be discarded.

KINEMATIC REJECTION CRITERIA (II)

The kinematic criteria for the event existence are to be established as follows. First, it is necessary to establish event types which will consist of the number of array stations and the number of non-array stations detecting. These stations may also have to be broken down by the criteria of analyst and automatic detection. For each type of event we may determine the ratio of good events to false events of each type in each day. This ratio then gives directly the probability that an event of each type is real.

PROCESSING AFTER DYNAMIC CHECKING

If any detections have been discarded then the reduced set of arrivals should be used to generate a new trial epicenter. If the same final set of arrivals should result then the iteration should be suspended. Care needs to be taken to avoid an infinite loop.

REFERENCES

Elvers, E. (1980). International Seismological Data Center: Procedures to check events through dynamic information and to estimate magnitudes, FOA Report C 20368-T1. Forsvarets Forskningsanstalt Huvudavdelning 2, Stockholm, Sweden.

Ringdal, F. (1976). Maximum likelihood estimation of seismic magnitude, Bull. Seism. Soc. Am., 66, 789-802.

Slunga, R. (1980). An algorithm for associating reported arrivals to a global seismic network into groups defining seismic events, FOA Report C 20386-T1, Forskningsanstalt Huvudavdelning 2, Stockholm, Sweden.

APPENDIX I

We have developed a Newton-Raphson algorithm for maximizing ln L(m) by noting that:

$$\frac{d \ln L(m)}{dm} = \frac{n_1}{\sigma_s^2}(\bar{m}-m) + \sum_{j=1}^{n_2} \frac{R(z_j)}{\omega_j} - \sum_{j=1}^{n_3} \frac{R(-z_j)}{\omega_j} \tag{A1}$$

where

$$R(z_j) = \frac{\phi(z_j)}{\Phi(z_j)} \tag{A2}$$

and

$$\omega_j = \sqrt{\sigma_s^2 + \sigma_j^2} \tag{A3}$$

where z_j given by the equation in the main text with:

$$\Phi(z) = \int_{-\infty}^{z} \phi(x)\, dx \tag{A4}$$

and

$$\phi(x) = (2\pi)^{-\frac{1}{2}} \exp\left(-\frac{x^2}{2}\right) \tag{A5}$$

Also:

$$\frac{\partial^2 \ln L(m)}{dm} = -\frac{n_1}{\sigma_s^2} - \sum_{j=1}^{n_2} \frac{(z_j R(z_j) + R^2(z_j))}{w_j^2} - \sum_{j=1}^{n_3} \frac{(z_j R(z_j) + R^2(-z_j))}{w_j^2}$$

Then the Newton-Raphson interations are of the form

$$m_{i+1} = m_i - \frac{\left(\frac{\partial \ln L(m)}{dm}\right)_{m_i}}{\left(\frac{\partial^2 \ln L(m)}{dm^2}\right)_{m_i}} \tag{A6}$$

with the final estimator $\hat{m}$ having an estimated standard error given by

$$\hat{\sigma}_{\hat{m}} = \left(- \frac{1}{\left(\frac{\partial^2 \ln L(m)}{dm^2}\right)_{\hat{m}}} \right)^{1/2} \tag{A7}$$

M E M O R A N D U M

TO: J. Goncz

FROM: R. Blandford RB

SUBJECT: A Better Approach to Handling Amplitude Data in AA

DATE: 19 April 1983

1. Compute maximum likelihood m_b using the observing stations plus a fixed set of about 20 reliable stations. An m_b is calculated with each station omitted in turn. Assume an a-priori $\sigma = 0.35\ m_b$ throughout.

2. Analyze each of the above stations in screen as we do now, get the total number of points, then:

   i. If the station did not detect but

   $$p(det) > .95,\ -1 \text{ point}$$
   $$p(det) > .99,\ -2 \text{ points}$$

   Comments: If p(det) > .95 at many stations most stations will have detected if the event is big and loss of points for the occasional random non-detection will not matter. If the event is weak, only a few close stations will have p(det) > 0.95 so the occasional random non-detection is again unlikely to lose points.

   ii. If the station did detect and if, based on noise and m_b alone

   $$p(det) < .01, -(\text{all points due to station})$$

   Comments: If the event is big there will be so many points that occasionally losing one will not be serious. If it is a small event and just trapped (correctly) the one distant station, then the probability of that happening for any particular one out of the 20 distant stations may be smaller than .05 so for that reason we set this threshold at .01 so that only about 1/5 of these events will be incorrectly rejected. It is important to reject all the points due to the station, i.e. those due to azimuth and slowness and those due to local flags and associated S phases.

   iii. If the station did detect, and reports an amplitude A_o, and if, based on noise and m_b alone,

   $$p(det) > .01 \text{ and}$$
   $$p(amp > A_o) < .01 \text{ or}$$
   $$p(amp < A_o) < .01 \text{ then}$$

discard amplitude, A_o (are left with estimated noise) and return to (1)

Comments: That is, compute all the negative points and m_b values over because the bad amplitude probably distorted all the m_b values. Note that this procedure does not "fiddle" with an event. It either results in complete acceptance or discards the event so that the kinematic processing has a new chance to do better.

RRB/paw

DISTRIBUTION LIST
(UNCLASSIFIED REPORTS)
DARPA FUNDED PROJECTS
(Last Revised 18 June 1984)

RECIPIENT	NUMBER OF COPIES
DEPARTMENT OF DEFENSE	
DARPA/GSD 1400 Wilson Boulevard Arlington, VA 22209	2
DARPA/PM 1400 Wilson Boulevard Arlington, VA 22209	1
Defense Technical Information Center Cameron Station Alexandria, VA 22314	12 2
Defense Intelligence Agency Directorate for Scientific and Technical Intelligence Washington, D.C. 20301	1
Defense Nuclear Agency Shock Physics Directorate/SS Washington, D.C. 20305	1
Defense Nuclear Agency/SPSS ATTN: Dr. Michael Shore 6801 Telegraph Road Alexandria, VA 22310	1
DEPARTMENT OF THE AIR FORCE	
AFGL/LW ATTN: Dr. J. Cipar Terrestrial Sciences Division Hanscom AFB, MA 01730	1
AFOSR/NPG ATTN: Director Bldg 410, Room C222 Bolling AFB, Washington D.C. 20332	1
AFTAC/TG Patrick AFB, FL 32925	3
AFTAC/TD (STINFO) Patrick AFB, FL 32925	1
AFWL/NTESC Kirtland AFB, NM 87171	1

DEPARTMENT OF THE ARMY

US Army Engineers 1
ATTN: Mr. J. Drake
Waterways Experiment Station
P.O. Box 631
Vicksburg, MS 39181

DEPARTMENT OF THE NAVY

NORDA 1
ATTN: Dr. J. A. Ballard
Code 543
NSTL Station, MS 39529

DEPARTMENT OF ENERGY

Department of Energy 1
ATTN: Dr. F. Dickerson (DP-52)
International Security Affairs
1000 Independence Avenue
Washington, D.C. 20545

Lawrence Livermore National Laboratory 2
ATTN: Dr. J. Hannon and Dr. M. Nordyke
University of California
P.O. Box 808
Livermore, CA 94550

Los Alamos Scientific Laboratory 1
ATTN: Dr. K. Olsen
P.O. Box 1663
Los Alamos, NM 87544

Sandia Laboratories 1
ATTN: Mr. P. Stokes
Geosciencies Department 1255
Albuquerque, NM 87115

OTHER GOVERNMENT AGENCIES

Central Intelligence Agency 1
ATTN: Dr. L. Turnbill
OSI/NED, Room 5G48
Washington, D.C. 20505

U.S. Arms Control and Disarmament Agency 2
ATTN: Mrs. M. Hoinkes
Division of Multilateral Affairs
Washington, D.C. 20301

U.S. Geological Survey 1
ATTN: Dr. T. Hanks
National Earthquake Research Center
345 Middlefield Road
Menlo Park, CA 94025

U.S. Geological Survey 1
ATTN: Dr. Robert Masse
Global Seismology Branch
Box 25046, Stop 967
Denver Federal Center
Denver, CO 80225

UNIVERSITIES

University of California, Berkeley 1
ATTN: DR. T. McEvilly
Department of Geology and Geophysics
Berkeley, CA 94720

California Institute of Technology 1
ATTN: Dr. D. Harkrider
Seismological Laboratory
Pasadena, CA 91125

University of California, San Diego 1
ATTN: Dr. J. Orcutt
Scripps Institute of Oceanography
La Jolla, CA 92093

Columbia University 1
ATTN: Dr. L. Sykes
Lamont-Doherty Geological Observatory
Palisades, NY 10964

Massachusetts Institute of Technology 3
ATTN: Dr. S. Soloman, Dr. N. Toksoz, Dr. T. Jordan
Department of Earth and Planetary Sciences
Cambridge, MA 02139

University of Nevada, Reno 1
ATTN: Dr. A. Ryall
Seismological Laboratory
Reno, NV 89557

The Pennsylvania State University 1
ATTN: Dr. S. Alexander
Department of Mineral Sciences
University Park, PN 16802

Southern Methodist University 1
ATTN: Dr. E. Herrin
Geophysical Laboratory
Dallas, TX 75275

CIRES 1
ATTN: Dr. C. Archambeau
University of Colorado
Boulder, CO 80309

Georgia Institute of Technology 1
ATTN: Professor Anton Dainty
The School of Geophysical Sciences
Atlanta, GA 30332

St. Louis University 1
ATTN: Dr. O. Nuttli
Department of Earth and Atmospheric Sciences
3507 Laclede
St. Louis, MO 63156

DEPARTMENT OF DEFENSE CONTRACTORS

Applied Research Associates, Incorporated 1
ATTN: Dr. N. Higgins
2101 San Pedro Boulevard North East
Suite A
Albuquerque, NM 87110

Applied Theory, Incorporated 1
ATTN: Dr. J. Trulio
930 South La Brea Avenue
Suite 2
Los Angeles, CA 90036

Center for Seismic Studies 2
ATTN: Dr. Carl Romney, and Dr. William Dean
1300 N. 17th Street, Suite 1450
Arlington, VA 22209

ENSCO, Incorporated 1
ATTN: Mr. G. Young
5408A Port Royal Road
Springfield, VA 22151

ENSCO, Incorporated 1
ATTN: Dr. R. Kemerait
1930 Highway A1A
Indian Harbour Beach, FL 32937

Pacific Sierra Research Corporation 1
ATTN: Mr. F. Thomas
12340 Santa Monica Boulevard
Los Angeles, CA 90025

Physics Applications, Incorporated 1
ATTN: Mr. C. Vincent
2340 Harris Way
San Jose, CA 95131

R&D Associates 1
ATTN: Dr. E. Martinelli
P.O. Box 9695
Marina del Rey, CA 90291

Rockwell International 1
ATTN: Dr. B. Tittmann
109 Camino.Dos Rios
Thousand Oaks, CA 91360

Gould Incorporated 1
ATTN: Mr. R. J. Woodard
Chesapeake Instrument Division
6711 Baymeado Drive
Glen Burnie, MD 21061

Rondout Associates, Incorporated 1
ATTN: Dr. P. Pomeroy
P.O. Box 224
Stone Ridge, NY 12484

Science Applications, Incorporated 1
ATTN: Dr. H. Pratt
P.O. Box 2351
La Jolla, CA 92038

Science Horizons
ATTN: Dr. T. Cherry and Dr. J. Minster 2
710 Encinitas Blvd
Suite 101
Encinitas, CA 92024

Sierra Geophysics, Incorporated 2
ATTN: Dr. R. Hart and Dr. G. Mellman
15446 Bell-Red Road
Redmond, WA 98052

SRI International 1
333 Ravensworth Avenue.
Menlo Park, CA 94025

S-Cubed
ATTN: Dr. Steven Day Dr. J. Savino 2
P.O. Box 1620
La Jolla, CA 92037

S-Cubed 1
ATTN: Mr. J. Murphy
11800 Sunrise Valley Drive
Suite 1112
Reston, VA 22091

Teledyne Geotech
ATTN: Dr. Z. Der and Mr. W. Rivers 2
314 Montgomery Street
Alexandria, VA 22314

Woodard-Clyde Associates 1
ATTN: Dr. Larry Burdick
380 West Del Mar Boulevard
Pasadena, CA 91105

Weidlinger Associates 1
ATTN: Dr. J. Isenberg
3000 Sand Hill Road
Building 4, Suite 245
Menlo Park, CA 94025

NON-U.S. RECIPIENTS

National Defense Research Institute 1
ATTN: Dr. Ola Dahlman
Stockholm 80, Sweden

Blacknest Seismological Center 1
ATTN: Mr. Peter Marshall
Atomic Weapons Research Establishment
UK Ministry of Defense
Brimpton, Reading RG7-4RS
United Kingdom

NTNF NORSAR 1
ATTN: Dr. Frode Ringdal
P.O. Box 51
N-2007 Kjeller
Norway

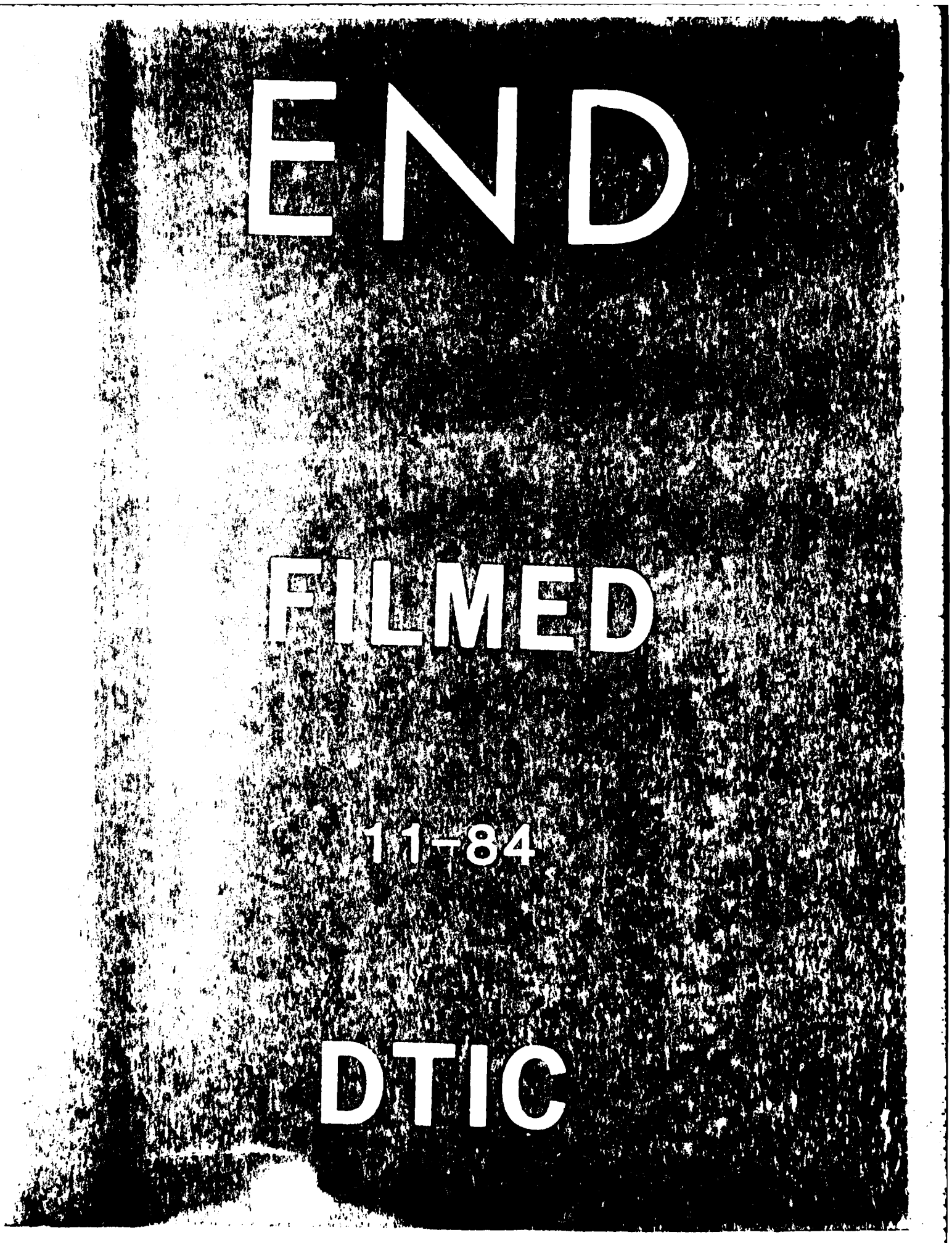
END
FILMED
11-84
DTIC